Dynamics and Vibration of the Stewart Platform, and Its Application in Vibration Isolation

A Thesis Submitted

in Partial Fulfillment of the Requirements

for the degree of

Master of Technology

by

Parthajit Mukherjee

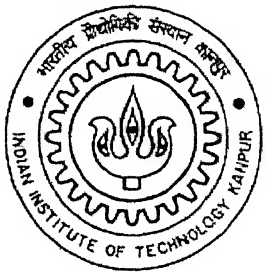

to the

Department of Mechanical Engineering

Indian Institute of Technology Kanpur

April, 2005

Dedicated to

My Parents and Grandfather

CERTIFICATE

It is certified that the work contained in this thesis entitled "**Dynamics and Vibration of the Stewart Platform, and Its Application in Vibration Isolation**," by **Mr. Parthajit Mukherjee (Roll No. Y3105050)**, has been carried out under our supervision and this work has not been submitted elsewhere for a degree.

21/04/05

Dr. Asok Kumar Mallik,
Professor,
Department of Mechanical Engineering,
Indian Institute of Technology Kanpur,
Kanpur, 208016.

Bhaskar Dasgupta
21/4/2005

Dr. Bhaskar Dasgupta,
Assistant Professor,
Department of Mechanical Engineering,
Indian Institute of Technology Kanpur,
Kanpur, 208016.

Abstract

This thesis attempts to develop a dynamic stability index of a general manipulator. It also deals with the analysis of dynamics and vibration of a 6-UPS Stewart platform. Finally, it presents a vibration control strategy for the same.

The dynamic formulation for a 6-UPS Stewart platform follows the Newton-Euler approach. Leg stiffness, force and torque due to viscous friction at the joints, inertia and gravity effects are considered in the model.

The response of the platform, subjected to disturbances at different frequencies, has been studied. A PD control strategy has then been proposed for controlling both free and forced vibrations and is applied to isolate the top platform from base vibrations.

Acknowledgments

I express my regards and sincere gratitude to my supervisors Prof. A. K. Mallik and Dr. B. Dasgupta for their excellent guidance, invaluable suggestions and generous help at all the stages of my research work. Their interest and confidence in me was the reason for the success I have achieved.

It was a great pleasure to be associated with the Center for Robotics and I would like to thank all the research engineers, staff members and my colleagues Rakesh, Auro, Siddhartha, Vivek, Omkar, Hari, Sivakanth, Rajkumar, Ekta and Ashish for encouraging me at every stage of my work and making the Center for Robotics a great place to work in.

I feel indebted to Indrani Kar for her invaluable suggestions regarding controllers. I am grateful to Shamik Chaudhuri for his academic and nonacademic help and involvement. I thank Vinod, Devendra Utsa, Krishnendu, Anik and Soumya for their support. I would also like to acknowledge the help of all of my classmates and friends at Hall - IV, who made my stay at IIT-Kanpur memorable.

Parthajit Mukherjee

Contents

List of Figures

Chapter 1

Introduction

1.1 Introduction

Technical applications resort to several instruments and machineries for achieving a concentrated objective. The sensitivity of the paraphernalia is a critical point requiring careful attention. The key natural phenomenon against which these need safeguarding is *vibrations.* Objects which require or generate motion are invariably subject to detrimental effects of vibration where a huge analytical effort is spent for eliminating or reducing it. Let us take the all-too-familiar example of a naval tracking camera. These are used for reconnaissance and target locking in ships. They are subjected to ship's motion viz. roll, pitch, etc. Similarly, reading of sensitive measuring instruments are affected by the vibrations of the shop-floor, caused by other machines. So, it is important to isolate these devices from surrounding disturbances. For active vibration isolation, the instruments can be put on the end-effector of a manipulator. The manipulator may be serial, parallel or hybrid in nature.

The advantage of serial manipulator is that its workspace is large. But due to cantilever nature, it is not very rigid and chatter is high. The links closer to base for a serial manipulator are subjected to the weight of the succeeding links in addition to the end-effector load. As a result, links are heavy for serial manipulators, rendering them unsuitable for high speed operations. High load and inertia also increase the requirement of power to drive them. Hence powerful motors are required for serial manipulators.

In parallel manipulators, the end-effector is supported and articulated by independent closed-loop kinematic chains. As the load is divided between the supporting links, each link has less inertia and motor power requirement is less stringent. Closed structural form

of parallel manipulators reduces chatter and deflections. Because of this reason and also accentuated by the fact that the inertia is less, they are suitable for high speed operations. Besides, for parallel manipulators, the end-effector can be positioned more precisely because the deflections are quite small. On the other hand, small workspace associated with parallel structures forms another issue in this field.

In some sense, the net motion at the end-effector, for a serial manipulator, is the summation of the individual link motions. On the other hand, end-effector force in parallel manipulators is the sum of individual link forces. Hybrid manipulators incorporate the advantages of both serial and parallel manipulators. They are made by combining serial structures in parallel or by parallel structures in serial manner or combinations thereof.

1.2 Comparison Between Serial and Parallel Manipulators

Each kinematic chain of parallel manipulators is constructed as a serial chain and hence they impose similar restrictions as serial manipulators. Therefore complex kinematic chain parallel manipulators cannot be compared in the following sense.

The most significant differences between a serial and a fully parallel manipulator are the following:

1. Degrees of freedom (DOF) of a serial manipulator is given by

$$\text{DOF} = \sum_{i=1}^{j} f_i$$

where f_i is the DOF of the i-th joint of the manipulator with a total number of j joints. For parallel manipulators, the expression of DOF is

$$\text{DOF} = m(n - j - 1) + \sum_{i=1}^{j} f_i$$

where n is the number of links and j is the number of joints. The DOF of a rigid body in the ambient space is denoted by m. It is 3 for planar and 6 for spatial manipulators, respectively.

2. Direct kinematics involves finding the position and orientation of the end-effector for given joint angles and is very simple and unique for serial manipulators. They can easily be obtained by using Denavit-Hartenberg parameters (D-H parameters) and homogeneous transformation matrices. For parallel manipulators direct kinematics is very complicated and requires a system of non-linear coupled algebraic equations to be solved. Moreover, direct kinematics is not unique for parallel manipulators.

   From the concept of serial-parallel duality, inverse kinematics is complicated and have multiple solutions for serial manipulators. But it is simpler and often gives unique solution for parallel manipulators.

3. The relation between joint velocities ($\dot{\Theta}$) and end-effector velocity ($\mathbf{V}$) for serial manipulators is given by,

$$\mathbf{V} = \mathbf{J}(\Theta)\dot{\Theta}$$

   where $\mathbf{J}(\Theta)$ is the *Jacobian matrix*. Its dual in parallel manipulator is *force transformation matrix* [$\mathbf{H}(\Theta)$]. It relates joint torques (τ) with the force supported by the manipulator ($\mathbf{F}$), in following manners,

$$\tau = \mathbf{H}(\Theta)\mathbf{F} \ .$$

   At singular configurations, the Jacobian matrix of serial manipulators becomes singular. Hence the end-effector loses one or more degrees-of-freedom making a part of the workspace inaccessible to the end-effector. On the contrary, at singular configurations, force transformation matrix of a parallel manipulator becomes singular. Hence it cannot support arbitrary load and gains one or more extra degrees of freedom.

4. Redundancy is incorporated into a serial manipulator to make it more dexterous. This increases the workspace and also gives it the ability to avoid obstacles to reach out for a particular TSL (task-space location). In spite of this, redundancy cannot *remove* the singularity of serial manipulators. Singularity only gets redistributed. Detailed discussions on redundancy can be found in works of Nakamura [38]. In parallel manipulators, redundancy improves its force supporting capabilities at the cost of workspace volume. Unlike serial manipulators, singularity of parallel manipulators can be reduced by incorporating redundancy. In certain cases, it can be successfully eliminated also. Dasgupta and Mrithyunjaya [6] have discussed it in detail.

5. Dynamics of serial manipulators are expressed in terms ordinary differential equations. In case of parallel manipulator these relations are exacerbated in complexity by constraints as they quite often turn out to be differential algebraic equations.

6. Control of serial manipulator is relatively simpler and can be done by proportional plus derivative (PD) control scheme. Control of parallel manipulator is much more complex due to nonlinear coupling.

1.3 Stewart Platform

Stewart platforms are most widely studied among the parallel manipulators. In general, Stewart platform can be described as two rigid bodies, namely base and top platforms, connected by six linearly actuated legs. Having six parallel-actuated simple kinematic chains, its DOF is also six. Connections between legs and platforms may be both spherical joints (called 6-SPS Stewart platform (Fig (1.1)) or one spherical and other universal joint (called 6-UPS Stewart platform (Fig (1.2)).

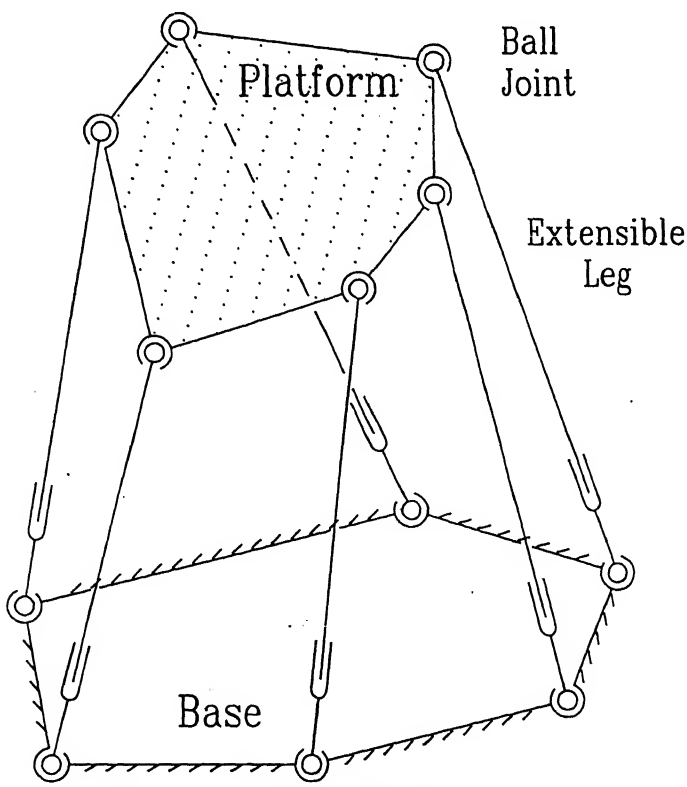

Figure 1.1: The 6 - SPS Stewart Platform

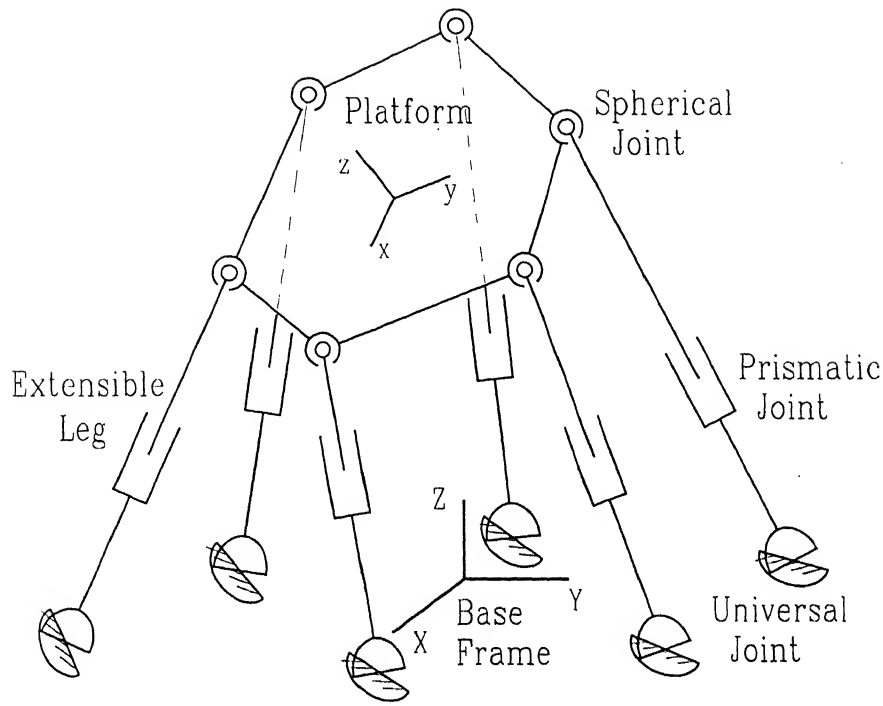

Figure 1.2: The 6 - UPS Stewart Platform

1.4 Literature Review

The Stewart platform derives its name from that of Stewart [35], who designed a mechanism for generating general motion for flight simulation. Gough suggested the use of six linear actuators in-parallel to actuate the platform [16]. McCallion and Truong first designed a Stewart platform for mechanical workstation [25]. They also performed some theoretical and numerical studies on mobility analysis and iterative solution of direct kinematics. Detailed study on workspace section and kinematics of Stewart platform were done by Merlet [29], Fichter [9], Yang and Lee [37].

Closed form dynamic equations of Stewart platform assuming rigid legs and stationary base were derived following three approaches viz. Newton-Euler method [5, 4], Lagrange method [19, 11] and virtual work principle [40].

Lee et al. [21] used Stewart platform for control purposes assuming legs to be rigid and base as fixed. Ren et al. [13] and Cheng et al. [2] used Stewart platform for isolating wind excited vibrations on a telescope mounted on a hanging cable car. They accounted for the

movement of the base but assumed components of the Stewart platform to be rigid. With the same assumptions, Kim and Lee [17] developed the mathematical model of Stewart platform for isolating a slender bar from the base excitation.

Shuguang and Schimmels [33] studied the behaviour of simple springs connected in parallel to a rigid body. Selig and Ding [32] developed a mathematical model of Stewart platform for the study of vibration, with simplified assumptions i.e. massless legs, frictionless passive joints. Lee and Geng [20] derived the dynamic model of Stewart platform by considering flexibility of its legs and assumed the base to be static. For micro-scale operations, McInroy [26] used flexure jointed hexapods. There he did not consider the inertia of the legs and assumed the base to be static. When we are interested in a particular position and it is pre-decided, the Stewart platform can be designed for this particular position. Geng and Haynes [12] have defined a special architecture of Stewart platform, which they termed as *'cubic configuration'*, where there is no coupling between the DOF of the Stewart platform. Hence, vibration control turns out to be simple at this configuration. Once it is fabricated, it can be used for this particular position and orientation only.

Basic study of singularities in parallel manipulators was done by Gosselin and Angeles [15]. They classified the singularities in 3 types. *'Singularity of 1st kind'* (motion singularity), *'singularity of 2nd kind'* (force singularity), *'singularity of 3rd kind'* (both singularities simultaneously). Stewart platform can have only *'singularity of 2nd kind'*. Later Ma and Angeles [23] showed that a highly symmetric Stewart platform (e.g. Stewart platform with regular hexagonal base and top platforms) is always singular. He called it *'architecture singularity'*. Gosselin [14] also studied singularity associated with high condition number of force transformation matrix. Bhattacharya et al. [1] and Dasgupta et al. [7] proposed strategies for singularity free path planning. They used a high condition number of force transformation matrix as the representation of singularity. In all these cases, singularity studies have taken into account the architecture and configuration (i.e. kinematic parameters) of Stewart platform. The dynamic parameters (i.e. mass, inertia, stiffness etc.) were not taken into account.

Yoshikawa [39] proposed *'dynamic manipulability ellipsoid'* (DME) to take care of the dynamic parameters of manipulators. It signifies, at a particular configuration how arbitrary change in acceleration of the end-effector can be obtained with joint driving forces. Though it

takes care of the inertia parameters of manipulator, it does not consider the stiffness. Ma and Angeles [22] have introduced *'dynamic conditioning index'* (DCI) and used it for designing manipulator for trajectory planning [24]. A low value of DCI signifies that the inertia matrix is close to ideal isotropic generalized inertia matrix. For an ideal isotropic generalized inertia matrix, inertia torques are completely decoupled, wherein they are easy to control.

1.5 Motivation and Scope of the Thesis

The previous section indicates that though kinematic and architectural singularities have been studied in great detail, effects of dynamic parameters have not received adequate attention. If the manipulator is used for control, it has to be dynamically stable. Hence there should be some well defined index for dynamic stability. Using Stewart platform as a representative, a dynamic stability index has been proposed in the 1st part of the present work.

The literature survey also indicates that, though detailed studies of dynamics of Stewart platform have been conducted considering fixed base and rigid legs, effect of moving base and flexible legs were not studied in great detail. In the second part of this work, completely general closed form dynamic equation of Stewart platform, following Newton-Euler approach, have been developed, considering the base movement and also accounting for the stiffness of the legs.

Subsequent to the above steps, we have employed PD control law to isolate the top platform from vibrations being transmitted from the base. Simulations have been performed using the closed form dynamic equations.

1.6 Thesis Organizations

In the next chapter, we develop a stability index which will take care of both kinematics and dynamics of manipulators. Comparisons of this with general singularity measure has been made through examples.

In chapter 3, completely general dynamic equations of Stewart platform have been developed using the Newton-Euler approach. In chapter 4, the stability index, developed in chapter 2, has been validated through numerical simulations.

In chapter 5, a linearized model, for gain selection, has been developed. For chosen values

of gains a PD control law is implemented to isolate the top platform from base vibrations and simulation results are included.

A summary of the work and future scopes have been discussed in chapter 6.

Chapter 2

Dynamic Stability Index

2.1 Introduction

From literature survey in Chapter 1, we observe that the effects of the dynamic parameters of a manipulator (i.e. mass, inertia, stiffness etc.) have not been taken into account for describing its stability. The natural frequencies, determined from linearized dynamic model of a manipulator, incorporate the contributions of all kinematic and dynamic parameters of the manipulator. Therefore, the lowest natural frequency may very well represent the stability of a manipulator. A low value of it signifies that the manipulator is tending towards *neutral stability*. Hence, it easily gets perturbed from desired position under small disturbances. These have been explained in this chapter by taking 6-UPS Stewart platform as an example.

In the next section, first we linearize the dynamic model to find out the natural frequencies. Then the sensitivity of the lowest natural frequency to dynamic parameters has been studied, taking numerical examples. Conclusions have been drawn from the simulation results.

2.2 Linearization of Dynamic Model of Stewart Platform for Free Vibration

We have assumed,

1. The base and top platforms are rigid.

2. Legs have lumped constant stiffness (due to hydraulic actuators, material compliance etc.) in axial direction. But they have no rotational stiffness.

The closed form dynamic equation of 6-UPS Stewart platform with fixed base in joint space [5] is

$$\mathbf{H}^{-1}\mathbf{J}\mathbf{H}^{-T}\ddot{\mathbf{L}} + \mathbf{H}^{-1}(\eta - \mathbf{J}\mathbf{H}^{-T}\mathbf{u}) = \mathbf{F} + \mathbf{H}^{-1}\begin{bmatrix} \Re\mathbf{F}_{ext} \\ \Re\mathbf{M}_{ext} \end{bmatrix}, \tag{2.1}$$

where

$\mathbf{J}$ = combined inertia of leg and moving platform.

$\mathbf{H}$ = input-output force transformation matrix.

η = force due to gravity, Coriolis acceleration and viscous friction at joints.

$\mathbf{F}$ = force, generated by actuators at the prismatic joint of legs or due to stiffness of legs.

$\mathbf{u}$ = centripetal acceleration of joining point of the moving platform and leg.

$\Re$ = rotation matrix specifying the orientation of the moving platform [3].

$\mathbf{F}_{ext}$ = resultant of external forces acting on the moving platform.

$\mathbf{M}_{ext}$ = resultant of external moments acting on the moving platform.

We are now interested only in the platform response to initial disturbances, so we can take external loads to be zero, without losing any generality. So, we get $\mathbf{F}_{ext} = \mathbf{M}_{ext} = \mathbf{0}$. For free vibration, magnitude of the force in i-th leg is

$$F_i = (K_{leg})_i(L_i - L_{0i}) = (K_{leg})_i\delta L_i \ , \tag{2.2}$$

where

L_{0i} = equilibrium length of i-th leg,

L_i = current length of i-th leg.

For free vibration, η and $\mathbf{u}$ are negligible compared to other terms of Eqn. (2.1). So combining Eqn. (2.1) and Eqn. (2.2) we get

$$\mathbf{H}^{-1}\mathbf{J}\mathbf{H}^{-T}\ddot{\mathbf{L}} = -\mathbf{K}\delta\mathbf{L} \ , \tag{2.3}$$

where

$$\mathbf{K} = \mathrm{diag}((K_{leg})_i).$$

Here $\mathbf{J}$ and $\mathbf{H}$ both depend on the constant properties of the platforms and legs (e.g. position of platform and base joints, mass and centre of mass of moving platform and legs etc.) as well as position and orientation ($\mathbf{t}$ and θ) of moving platform. So, natural frequencies and mode shapes of Stewart platform also depend on position and orientation. For a particular position and orientation of a given Stewart platform , both $\mathbf{J}$ and $\mathbf{H}$ are constants. Hence $\mathbf{H}^{-1}\mathbf{J}\mathbf{H}^{-T}$ is constant for that position and orientation. We denote $\mathbf{H}^{-1}\mathbf{J}\mathbf{H}^{-T}$ as $\mathbf{J}_0$. So Eqn. (2.3) becomes,

$$\mathbf{J}_0\ddot{\mathbf{L}} = -\mathbf{K}\delta\mathbf{L}. \tag{2.4}$$

Assuming $\mathbf{L}e^{i\omega t}$ to be a solution of the Eqn. (2.4), we get the a generalized eigenvalue problem [31]

$$\omega^2\mathbf{J}_0\mathbf{L} = \mathbf{K}\mathbf{L}. \tag{2.5}$$

Solving Eqn. (2.5) we get *six* natural frequencies and *six* mode shapes [28, 27, 36] for a particular position and orientation of the Stewart platform.

The lowest natural frequency, calculated from Eqn. (2.5), is an index for dynamic stability of the manipulator. When the value of the lowest natural frequency is zero, the manipulator becomes neutrally stable, and hence, it cannot restore its position and orientation if it is perturbed by any amount. A very low value also signifies dynamic instability of the manipulator. Therefore, the lowest natural frequency plays the same role in dynamic stability as does the condition number of the force transformation matrix in statics. High value of the condition number of the force transformation matrix signifies the static singularity of the manipulator.

2.3 Simulation

The generalized eigenvalue problem (Eqn. 2.5) has been solved in **MATLAB**, taking two sets of numerical values for two different designs of Stewart platform. Between them, one is completely general [5] and other one is designed for minimum condition number of $\mathbf{H}$ [8]. The variation of the lowest natural frequency with condition number of $\mathbf{H}$ for different mass of the moving platform (M) is shown in Figs. (2.1) - (2.4). Suitable stiffnesses of the legs for both the cases and dynamic parameters for second case have been assumed. The values of the parameters are given in the appendix A.

For different position and orientation of Stewart platform, though the condition number

of **H** may be same, the lowest natural frequency may be different. This can be seen from the plots also.

1. **Example: 1**

   (a) **Case: 1 M = 40 kg.** (b) **Case: 2 M = 4000 kg.**

2. **Example: 2**

   (a) **Case: 1 M = 4 kg.** (b) **Case: 2 M = 400 kg.**

In Figs. (2.1) - (2.4) we can see that the lowest natural frequency of Stewart platform decreases very sharply with increase of condition number of **H**. As **H** tends towards ill-conditioning, the platform cannot support load coming from certain directions. Therefore, it gains one or more degrees of freedom. Very low value of the lowest natural frequency also signifies the instability of the moving platform.

But, at the same condition number of **H**, at different poses (different position and orientation), we see a lot of variation of the lowest natural frequency. Here, condition number of **H** alone cannot point out which position and orientation is more stable.

With the same kinematic parameters, but with different mass of the moving platform, variation of the lowest natural frequency is significant. With the change of mass of the top platform, drastic change of the lowest natural frequency of the test manipulator I, is clear from Fig. (2.1) and Fig. (2.2). Similarly, the variation of the lowest natural frequency of the test manipulator II, can be seen in Fig. (2.3) and Fig. (2.4). In both the cases, the lowest natural frequency decreases sharply with increasing mass of the platform, which signifies increasing dynamic instability of the moving platform. This effect also cannot be explained with the condition number of **H**.

2.4 Conclusions

From the plots and the discussion in the previous section we can make following conclusions.

1. Where *dynamic stability is more important, design criterion can be maximization of the lowest natural frequency.* When we are interested in different positions and orientations,

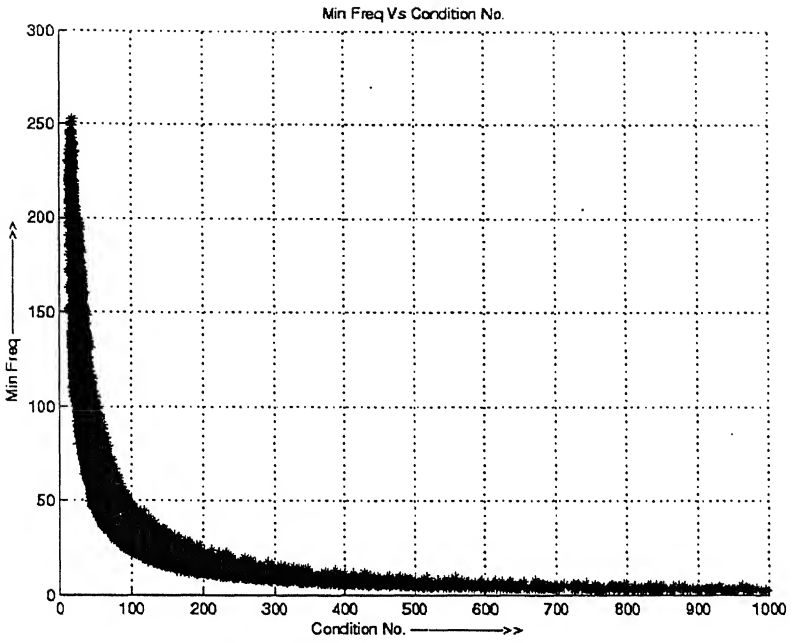

Figure 2.1: (Ex: 1, Case: 1) Minimum Natural Frequency Vs. Condition Number of **H**

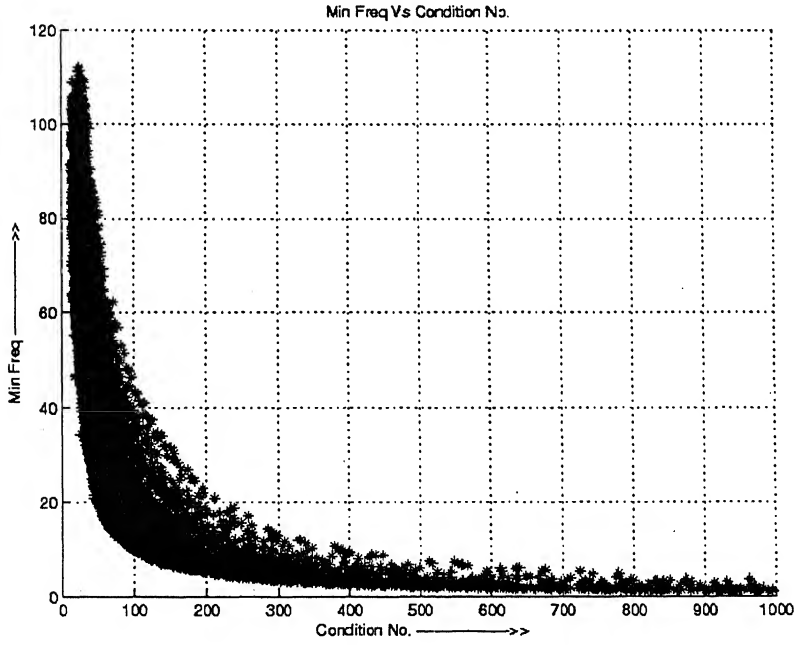

Figure 2.2: (Ex: 1, Case: 2) Minimum Natural Frequency Vs. Condition Number of **H**

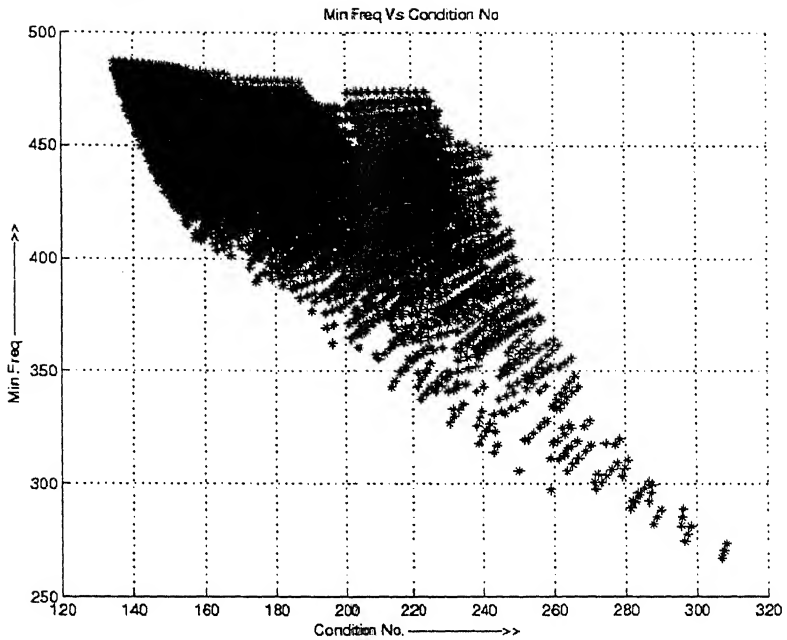

Figure 2.3: (Ex: 2, Case: 1) Minimum Natural Frequency Vs. Condition Number of **H**

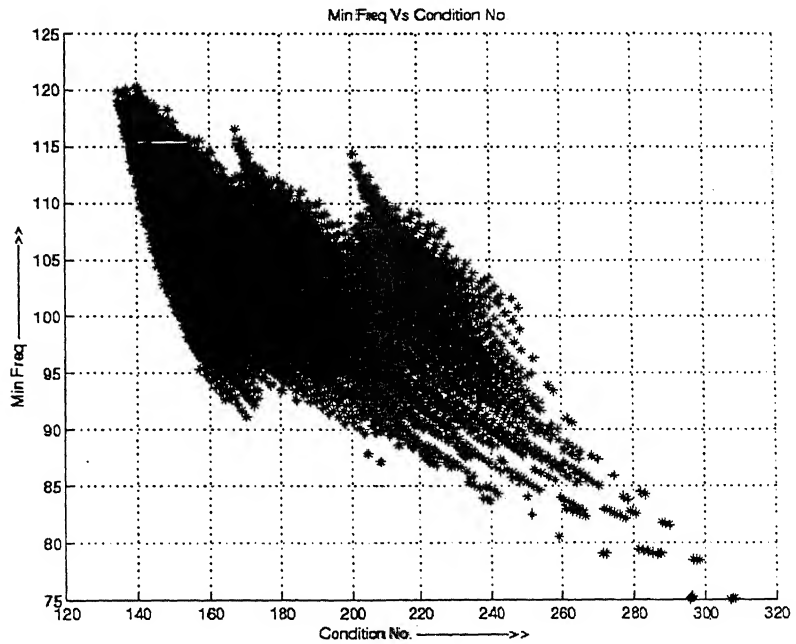

Figure 2.4: (Ex: 2, Case: 2) Minimum Natural Frequency Vs. Condition Number of **H**

instead of a particular one, i.e. if the manipulator is going to be used in a path planning and tracking purpose, the design criterion can be that the lowest natural frequency is higher than a lower bound over the entire path or it should be maximized over the path in a cumulative sense with some appropriate weights. Here, more stringent first criterion needs more computation resources and also requires robust optimization routine to solve them. Little relaxation of the requirements can be done by following the second criterion. But in this case, appropriate weights should be decided based on the criticality of the operation. Over the whole path if there are some poses where manipulator needs to be made more stable from the application point of view, weights should be high for these poses.

2. The natural frequencies are also important for choosing the gains of PD controller. *Gains should be chosen in such a way so that the close loop poles of the corresponding linearized system* (linearized model has been given in chapter 5) *should not fall near the natural frequencies.* If they fall near the natural frequencies, the controlled system will vibrate more than the uncontrolled one.

3. From the natural frequencies, we get a rough estimation of the sampling time (Δt) for controller. For proper control, sampling time should be $\Delta t = \frac{2\pi}{20\omega_{n_{max}}}$ [10]. Where, $\omega_{n_{max}}$ is the highest natural frequency.

Chapter 3

Closed Form Dynamic Equation of Stewart Platform with Base Motions and Flexible Legs

3.1 Introduction

Dynamics of Stewart platform is quite complicated due to its closed chain construction and six degrees of freedom. From literature survey, we find that a good amount of research has been pursued to find out closed form dynamic equations of Stewart platform, following both the Newton-Euler and the Lagrangian approaches. But the effects of base motion and flexibility of the legs have not been throughly explored. Use of a completely general dynamic model will give better performance of the controller. In this chapter, a generalized dynamic model of a 6-UPS Stewart platform following the Newton-Euler approach has been developed in the same way as by Dasgupta and Mrithyunjaya [4, 5]. Base motion, friction at the joints, inertia of legs and platform, flexibility of the legs are also considered in the model. Leg stiffness, present only in axial direction, is assumed to be lumped.

3.2 Closed Form Dynamic Equations for 6-UPS Stewart Platform

To develop closed form dynamic equations, first kinematics and dynamics of the legs have been studied. Then the force, applied on the top platform by each leg, and the external loads have been combined to formulate the dynamic equations of the top platform in task space.

While deriving the equations of motion for a leg, the suffix i, denoting a general leg, is omitted to reduce the cluttering of the equations with too many indices. From the context, it is quite clear that this equation is for a general leg. At the time of writing equations for the platform, the suffix i has been incorporated.

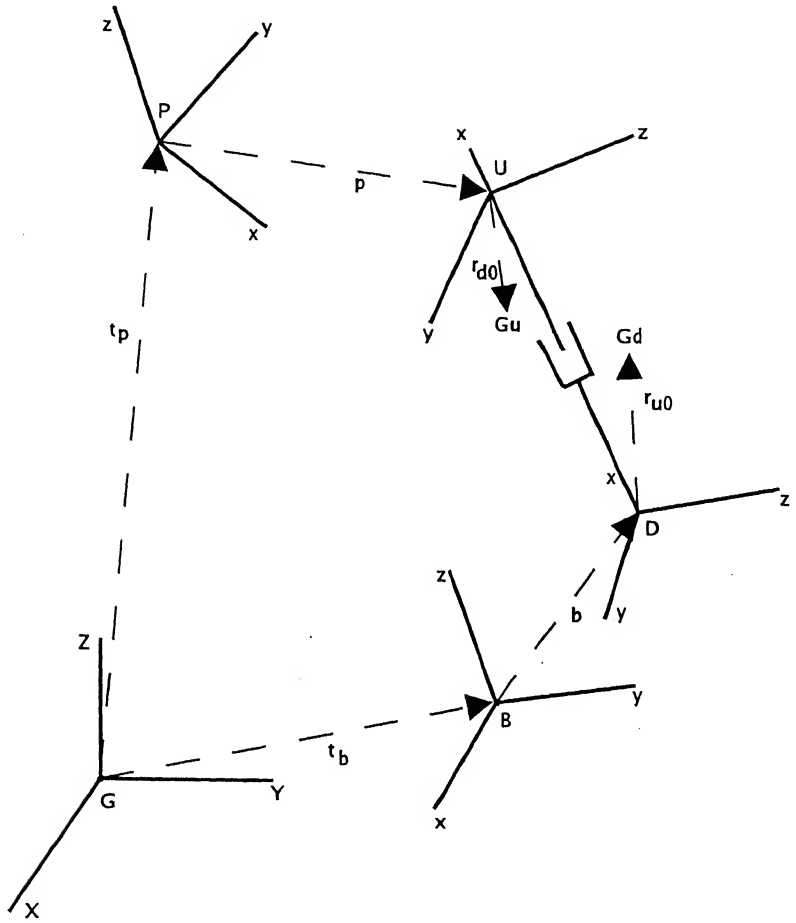

Figure 3.1: Positions of Reference Frames

The detailed diagram depicting different reference frames and a schematic leg is shown in Fig. (3.1). The symbols used to develop the model are explained below:

$\mathbf{G}$ = global inertial reference frame.

$\mathbf{B}$ = base frame (attached to the reference point of the base platform).

$\mathbf{P}$ = platform frame (attached to the reference point of the top platform).

$\mathbf{D, U}$ = Frames, attached to lower and upper part of the legs, respectively.

$\mathbf{t}_b$ = position of the frame **B** with respect to frame **G**.

$\mathbf{t}_p$ = position of the frame **P** with respect to frame **G**.

$\Re_b$ = rotation matrix (orientation of the frame **B** w.r.t. frame **G**).

$\Re_p$ = rotation matrix (orientation of the frame **P** w.r.t. frame **G**).

$\mathbf{b}_i$ = i-th base point in the base frame.

$\mathbf{p}_i$ = i-th platform point in the platform frame.

$\mathbf{q_{b}}_i$ = $\Re_b \mathbf{b}_i$.

$\mathbf{q_{p}}_i$ = $\Re_p \mathbf{p}_i$.

$\dot{\mathbf{t}}_b$ = linear velocity of the base platform w.r.t. frame **G**.

$\dot{\mathbf{t}}_p$ = linear velocity of the top platform w.r.t. frame **G**.

ω_b = angular velocity of the base platform w.r.t. frame **G**.

ω_p = angular velocity of the top platform w.r.t. frame **G**.

$\ddot{\mathbf{t}}_b$ = linear acceleration of the base platform w.r.t. frame **G**.

$\ddot{\mathbf{t}}_p$ = linear acceleration of the top platform w.r.t. frame **G**.

α_b = angular acceleration of the base platform w.r.t. frame **G**.

α_p = angular acceleration of the top platform w.r.t. frame **G**.

$\mathbf{R}_{0p}$ = centre of gravity of the top platform in platform frame.

M = mass of the top platform including payload.

$\mathbf{I}_p$ = moment of inertia of the top platform including payload in platform frame.

$\mathbf{F}_{ext}$ = external force on the top platform in the platform frame.

$\mathbf{M}_{ext}$ = external moment on the top platform in the platform frame.

$\bar{\mathbf{k}}_i$ = stationary axis of the universal joint at i-th leg.

$\mathbf{T}_i$ = rotation matrix (orientation) of i-th leg w.r.t. frame **G**.

$(m_d)_i, (m_u)_i$ = masses of the lower and upper part of i-th leg.

$(\mathbf{r}_{d_0})_i, (\mathbf{r}_{u_0})_i$ = centre of gravity of the lower and upper part of i-th leg in local frames.

$(\mathbf{I}_{d_0})_i, (\mathbf{I}_{u_0})_i$ = Moments of inertia of lower and upper part of i-th leg in local frames.

$\mathbf{g}$ = acceleration due to gravity.

C_u, Cp, C_s = coefficients of friction in the universal, prismatic and spherical joints respectively.

F_i = magnitude of input force at i-th leg.

$\mathbf{S}_i$ = vector along i-th leg.

3.2.1 Velocity Analysis of i-th Leg

Vector along i-th leg:

$$\mathbf{S} = (\mathbf{q_p} + \mathbf{t}_p) - (\mathbf{q_b} + \mathbf{t}_b). \tag{3.1}$$

Hence leg length:

$$L = \| \mathbf{S} \| . \tag{3.2}$$

Unit vector along the leg:

$$\mathbf{s} = \mathbf{S}/L. \tag{3.3}$$

$$\mathbf{T} = [\hat{\mathbf{x}} \quad \hat{\mathbf{y}} \quad \hat{\mathbf{z}}], \tag{3.4}$$

where

$$\mathbf{k} = \Re_b \overline{\mathbf{k}} \quad \text{and} \quad \hat{\mathbf{x}} = \mathbf{s}; \quad \hat{\mathbf{y}} = (\mathbf{k} \times \mathbf{s}) / \| \mathbf{k} \times \mathbf{s} \|; \quad \hat{\mathbf{z}} = \hat{\mathbf{x}} \times \hat{\mathbf{y}}.$$

Centres of gravity of lower and upper part w.r.t. global reference frame:

$$\mathbf{r}_d = \mathbf{T}\mathbf{r}_{d_0}, \tag{3.5}$$

$$\mathbf{r}_u = \mathbf{T}(\mathbf{v} + \mathbf{r}_{u_0}), \tag{3.6}$$

where

$$\mathbf{v} = [L \quad 0 \quad 0]^T.$$

Moments of inertia of the lower and upper part w.r.t. global reference frame:

$$\mathbf{I}_d = \mathbf{T}\mathbf{I}_{d_0}\mathbf{T}^T, \tag{3.7}$$

$$\mathbf{I}_u = \mathbf{T}[\mathbf{I}_{u_0} + m_u L^2 \mathrm{diag}(0,1,1)]\mathbf{T}^T. \tag{3.8}$$

Relative velocity between the base point and platform point:

$$\dot{\mathbf{S}} = (\omega_p \times \mathbf{q}_p + \dot{\mathbf{t}}_p) - (\omega_b \times \mathbf{q}_b + \dot{\mathbf{t}}_b). \tag{3.9}$$

Hence relative sliding velocity between upper and lower part of the leg:

$$\dot{L} = \mathbf{s} \cdot \dot{\mathbf{S}}. \tag{3.10}$$

Angular velocity of the leg:

$$\mathbf{W} = \mathbf{s} \times \dot{\mathbf{S}}/L. \tag{3.11}$$

3.2.2 Acceleration Analysis of i-th Leg

The relative acceleration between the base point and platform point:

$$\ddot{\mathbf{S}} = [\ddot{\mathbf{t}}_p + \alpha_p \times \mathbf{q}_p + \omega_p \times (\omega_p \times \mathbf{q}_p)] - [\ddot{\mathbf{t}}_b + \alpha_b \times \mathbf{q}_b + \omega_b \times (\omega_b \times \mathbf{q}_b)]. \tag{3.12}$$

Let us group the velocity dependent terms in $\mathbf{U}_1$ and the acceleration dependent terms in $\mathbf{a}_p$ and $\mathbf{a}_b$, as

$$\mathbf{U}_1 = \omega_p \times (\omega_p \times \mathbf{q}_p) - \omega_b \times (\omega_b \times \mathbf{q}_b), \tag{3.13}$$

$$\mathbf{a}_p = \ddot{\mathbf{t}}_p + \alpha_p \times \mathbf{q}_p, \quad \text{and} \tag{3.14}$$

$$\mathbf{a}_b = \ddot{\mathbf{t}}_b + \alpha_b \times \mathbf{q}_b. \tag{3.15}$$

Hence, $\ddot{\mathbf{S}}$ becomes

$$\ddot{\mathbf{S}} = \mathbf{a}_p - \mathbf{a}_b + \mathbf{U}_1. \tag{3.16}$$

$\ddot{\mathbf{S}}$ can be expressed in terms of leg quantities like relative sliding acceleration, angular velocity and angular acceleration as,

$$\ddot{\mathbf{S}} = \ddot{L}\mathbf{s} + \mathbf{W} \times (\mathbf{W} \times \mathbf{S}) + 2\mathbf{W} \times \dot{L}\mathbf{s} + \mathbf{A} \times \mathbf{S}. \tag{3.17}$$

Presence of a universal joint, at one end of the leg, inhibits its rotation about its own axis along the length. Therefore, $\mathbf{W} \cdot \mathbf{s}$ and $\mathbf{A} \cdot \mathbf{s}$ are zero. Equating $\ddot{\mathbf{S}} \cdot \mathbf{s}$ from equations (3.16) and (3.17) and using the relation $\mathbf{W} \cdot \mathbf{s} = 0$, we get

$$\ddot{L} = \mathbf{s} \cdot (\mathbf{a}_p - \mathbf{a}_b) + u \tag{3.18}$$

where

$$u = \mathbf{s} \cdot \mathbf{U}_1 + \frac{1}{L}(\dot{\mathbf{S}} - \dot{L}\mathbf{s})^2. \tag{3.19}$$

Similarly equating $\mathbf{s} \times \ddot{\mathbf{S}}$ from both equations (3.16) and (3.17) along with the relations $\mathbf{W} \cdot \mathbf{s} = 0$ and $\mathbf{A} \cdot \mathbf{s} = 0$ we get

$$\mathbf{A} = \frac{1}{L}\mathbf{s} \times (\mathbf{a}_p - \mathbf{a}_b) + \mathbf{U}_2 \tag{3.20}$$

where

$$\mathbf{U}_2 = \frac{1}{L}(\mathbf{s} \times \mathbf{U}_1 - 2\dot{L}\mathbf{W}). \tag{3.21}$$

Accelerations of centre of gravity of lower and upper parts of the leg are respectively,

$$\mathbf{a}_d = [\ddot{\mathbf{t}}_b + \alpha_b \times \mathbf{q}_b + \omega_b \times (\omega_b \times \mathbf{q}_b)] + \mathbf{A} \times \mathbf{r}_d + \mathbf{W} \times (\mathbf{W} \times \mathbf{r}_d), \tag{3.22}$$

$$\mathbf{a}_u = [\ddot{\mathbf{t}}_b + \alpha_b \times \mathbf{q}_b + \omega_b \times (\omega_b \times \mathbf{q}_b)] + \ddot{L}\mathbf{s} + \mathbf{A} \times \mathbf{r}_u + \mathbf{W} \times (\mathbf{W} \times \mathbf{r}_u) + 2\dot{L}\mathbf{W} \times \mathbf{s}. \tag{3.23}$$

Simplifying and using Eqn. (3.20), we get

$$\mathbf{a}_d = \frac{1}{L}(\mathbf{s} \times \mathbf{a}_p) \times \mathbf{r}_d + [\mathbf{a}_b - \frac{1}{L}(\mathbf{s} \times \mathbf{a}_b) \times \mathbf{r}_d] + \mathbf{U}_3 \tag{3.24}$$

$$\mathbf{a}_u = (\mathbf{s} \cdot \mathbf{a}_p)\mathbf{s} + \frac{1}{L}(\mathbf{s} \times \mathbf{a}_p) \times \mathbf{r}_u + [\mathbf{a}_b - \frac{1}{L}(\mathbf{s} \times \mathbf{a}_b) \times \mathbf{r}_u - (\mathbf{s} \cdot \mathbf{a}_b)\mathbf{s}] + \mathbf{U}_4 \tag{3.25}$$

where

$$\mathbf{U}_3 = \mathbf{U}_2 \times \mathbf{r}_d + \mathbf{W} \times (\mathbf{W} \times \mathbf{r}_d) + \omega_b \times (\omega_b \times \mathbf{q}_b) \tag{3.26}$$

$$\mathbf{U}_4 = u\mathbf{s} + \mathbf{U}_2 \times \mathbf{r}_u + \mathbf{W} \times (\mathbf{W} \times \mathbf{r}_u) + 2\dot{L}\mathbf{W} \times \mathbf{s} + \omega_b \times (\omega_b \times \mathbf{q}_b) \tag{3.27}$$

3.2.3 Dynamics of i-th Leg

If $\mathbf{F}_s$ is the force acting on the leg at the spherical joint, from moment equilibrium of the entire leg, we get

$$-m_d\mathbf{r}_d \times \mathbf{a}_d - m_u\mathbf{r}_u \times \mathbf{a}_u + (m_d\mathbf{r}_d + m_u\mathbf{r}_u) \times \mathbf{g} - (\mathbf{I}_d + \mathbf{I}_u)\mathbf{A} - \mathbf{W} \times (\mathbf{I}_d + \mathbf{I}_u)\mathbf{W} + M_u\mathbf{s} + \mathbf{S} \times \mathbf{F}_s - C_u\mathbf{W} - \mathbf{f} = \mathbf{0} \tag{3.28}$$

or,

$$M_u\mathbf{s} + \mathbf{S} \times \mathbf{F}_s = \mathbf{C} \tag{3.29}$$

where

$$\mathbf{C} = m_d\mathbf{r}_d \times \mathbf{a}_d + m_u\mathbf{r}_u \times \mathbf{a}_u - (m_d\mathbf{r}_d + m_u\mathbf{r}_u) \times \mathbf{g} + (\mathbf{I}_d + \mathbf{I}_u)\mathbf{A} + \mathbf{W} \times (\mathbf{I}_d + \mathbf{I}_u)\mathbf{W} + C_u\mathbf{W} + \mathbf{f}. \tag{3.30}$$

The expression of $\mathbf{f}$, the moment acting at the spherical joint due to viscous friction, is

$$\mathbf{f} = C_s(\mathbf{W} - \omega_p). \tag{3.31}$$

Taking cross product of both the sides of Eqn. (3.29) with $\mathbf{s}$ and rearranging, we get

$$\mathbf{F}_s = (\mathbf{s} \cdot \mathbf{F}_s)\mathbf{s} + \frac{1}{L}\mathbf{C} \times \mathbf{s}. \tag{3.32}$$

From the force-equilibrium along the axis of the leg,

$$F + \mathbf{s} \cdot \mathbf{F}_s - C_p\dot{L} + m_u\mathbf{s} \cdot \mathbf{g} = m_u\mathbf{s} \cdot \mathbf{a}_u. \tag{3.33}$$

Substituting $\mathbf{s} \cdot \mathbf{F}_s$ from Eqn. (3.33) into Eqn. (3.32) and using Eqns. (3.20), (3.26), (3.27) and (3.30) we get,

$$\begin{aligned}
\mathbf{F}_s &= m_u[\mathbf{s} \cdot \mathbf{a}_p + \frac{1}{L}\{(\mathbf{s} \cdot \mathbf{r}_u)\mathbf{s} \cdot \mathbf{a}_p - \mathbf{r}_u \cdot \mathbf{a}_p\} - \frac{1}{L}\{(\mathbf{s} \cdot \mathbf{r}_u)\mathbf{s} \cdot \mathbf{a}_b - \mathbf{r}_u \cdot \mathbf{a}_b\}]\mathbf{s} \\
&\quad -\frac{1}{L}\mathbf{s} \times [m_d\mathbf{r}_d \times \{\frac{1}{L}(\mathbf{s} \times \mathbf{a}_p) \times \mathbf{r}_d + (\mathbf{a}_b - \frac{1}{L}(\mathbf{s} \times \mathbf{a}_b) \times \mathbf{r}_d) \\
&\quad +m_u\mathbf{r}_u \times \{(\mathbf{s} \cdot \mathbf{a}_p)\mathbf{s} + \frac{1}{L}(\mathbf{s} \times \mathbf{a}_p) \times \mathbf{r}_u + (\mathbf{a}_b - \frac{1}{L}(\mathbf{s} \times \mathbf{a}_b) \times \mathbf{r}_u - (\mathbf{s} \cdot \mathbf{a}_b)\mathbf{s})\} \\
&\quad +\frac{1}{L}(\mathbf{I}_d + \mathbf{I}_u)\mathbf{s} \times (\mathbf{a}_p - \mathbf{a}_b)] + \mathbf{V} - \mathbf{s}F
\end{aligned} \tag{3.34}$$

where

$$\mathbf{V} = (m_u\mathbf{s} \cdot \mathbf{U}_4 + C_p\dot{L} - m_u\mathbf{s} \cdot \mathbf{g})\mathbf{s} - \frac{1}{L}\mathbf{s} \times \mathbf{U}_5 \tag{3.35}$$

and

$$\begin{aligned}
\mathbf{U}_5 &= m_d\mathbf{r}_d \times \mathbf{U}_3 + m_u\mathbf{r}_u \times \mathbf{U}_4 + (\mathbf{I}_d + \mathbf{I}_u)\mathbf{U}_2 \\
&\quad +\mathbf{W} \times (\mathbf{I}_d + \mathbf{I}_u)\mathbf{W} - (m_d\mathbf{r}_d + m_u\mathbf{r}_u) \times \mathbf{g} + C_u\mathbf{W} + \mathbf{f}.
\end{aligned} \tag{3.36}$$

Eqn. (3.34) can be written in compact form:

$$\mathbf{F}_s = \mathbf{Q}_p\mathbf{a}_p - \mathbf{Q}_b\mathbf{a}_b + \mathbf{V} - \mathbf{s}F \tag{3.37}$$

where

$$\begin{aligned}
\mathbf{Q}_p &= [m_u(1 + \frac{2\mathbf{s} \cdot \mathbf{r}_u}{L}) - \frac{m_dr_d^2 + m_ur_u^2}{L^2}]\mathbf{s}\mathbf{s}^T + \frac{m_dr_d^2 + m_ur_u^2}{L}\mathbf{E}_3 - \frac{m_u}{L}(\mathbf{s}\mathbf{r}_u^T + \mathbf{r}_u\mathbf{s}^T) \\
&\quad -\frac{1}{L^2}[m_d(\mathbf{s} \times \mathbf{r}_d)(\mathbf{s} \times \mathbf{r}_d)^T + m_u(\mathbf{s} \times \mathbf{r}_u)(\mathbf{s} \times \mathbf{r}_u)^T + \tilde{\mathbf{s}}(\mathbf{I}_d + \mathbf{I}_u)\tilde{\mathbf{s}}]
\end{aligned} \tag{3.38}$$

$$\begin{aligned}
\mathbf{Q}_b &= [m_u\frac{\mathbf{s} \cdot \mathbf{r}_u}{L} - \frac{m_dr_d^2 + m_ur_u^2}{L^2}]\mathbf{s}\mathbf{s}^T + \frac{m_dr_d^2 + m_ur_u^2}{L}\mathbf{E}_3 - \frac{m_u}{L}(\mathbf{s}\mathbf{r}_u^T + \mathbf{s}^T\mathbf{r}_u\mathbf{E}_3) \\
&\quad +\frac{m_d}{L}(\mathbf{r}_d\mathbf{s}^T - \mathbf{s}^T\mathbf{r}_d\mathbf{E}_3) - \frac{1}{L^2}[m_d(\mathbf{s} \times \mathbf{r}_d)(\mathbf{s} \times \mathbf{r}_d)^T \\
&\quad +m_u(\mathbf{s} \times \mathbf{r}_u)(\mathbf{s} \times \mathbf{r}_u)^T + \tilde{\mathbf{s}}(\mathbf{I}_d + \mathbf{I}_u)\tilde{\mathbf{s}}]
\end{aligned} \tag{3.39}$$

$\mathbf{E}_3$ is the 3×3 identity matrix and

$$\tilde{\mathbf{s}} = \begin{bmatrix} 0 & -s_z & s_y \\ s_z & 0 & -s_x \\ -s_y & s_x & 0 \end{bmatrix}$$

Now substituting expressions for $\mathbf{a}_p$ and $\mathbf{a}_b$ from Eqns. (3.14) and (3.15), respectively, into Eqn. (3.37) and simplifying, we get the expression of force acting at spherical joint of i-th leg as

$$(\mathbf{F}_s)_i = (\mathbf{Q}_{\mathbf{p}_i}\ddot{\mathbf{t}}_p - \mathbf{Q}_{\mathbf{b}_i}\ddot{\mathbf{t}}_b) - (\mathbf{Q}_{\mathbf{p}_i}\tilde{\mathbf{q}}_{\mathbf{p}_i}\alpha_p - \mathbf{Q}_{\mathbf{b}_i}\tilde{\mathbf{q}}_{\mathbf{b}_i}\alpha_b) + \mathbf{V}_i - \mathbf{s}_i F_i. \tag{3.40}$$

3.2.4 Kinematics of Top platform

Position vector of center of gravity of top platform in global reference frame is

$$\mathbf{R}_p = \Re_p \mathbf{R}_{0p}. \tag{3.41}$$

The acceleration of top platform in global reference frame is

$$\mathbf{a} = \ddot{\mathbf{t}}_p + \omega_p \times (\omega_p \times \mathbf{R}_p) + \alpha_p \times \mathbf{R}_p. \tag{3.42}$$

The moment of inertia of top platform including payload in global reference frame is

$$\mathbf{I} = \Re_p \mathbf{I}_p \Re_p^T. \tag{3.43}$$

3.2.5 Dynamics of Platform in Task-Space

From force balance of top platform, we get

$$-M\mathbf{a} + M\mathbf{g} + \Re_p \mathbf{F}_{ext} - \sum_{i=1}^{6} (\mathbf{F}_s)_i = \mathbf{0}. \tag{3.44}$$

Substituting expressions of $\mathbf{a}$ and $(\mathbf{F}_s)_i$ from Eqns. (3.42) and (3.40) into Eqn. (3.44) and simplifying we get

$$\begin{aligned}(M\mathbf{E}_3 + \sum_{i=1}^{6} \mathbf{Q}_{\mathbf{p}_i})\ddot{\mathbf{t}}_p - (M\tilde{\mathbf{R}}_p + \sum_{i=1}^{6} \mathbf{Q}_{\mathbf{p}_i}\tilde{\mathbf{q}}_{\mathbf{p}_i})\alpha_p - \sum_{i=1}^{6} \mathbf{Q}_{\mathbf{b}_i}\ddot{\mathbf{t}}_b \\ + \sum_{i=1}^{6} \mathbf{Q}_{\mathbf{b}_i}\tilde{\mathbf{q}}_{\mathbf{b}_i}\alpha_b + M\{\omega_p \times (\omega_p \times \mathbf{R}_p) - \mathbf{g}\} + \sum_{i=1}^{6} \mathbf{V}_i \;=\; \sum_{i=1}^{6} \mathbf{s}_i F_i + \Re_p \mathbf{F}_{ext}.\end{aligned} \tag{3.45}$$

Using Euler's equation for platform about the platform reference point we get,

$$
\begin{aligned}
-M\mathbf{R}_p \times [\ddot{\mathbf{t}}_p + \alpha_p \times \mathbf{R}_p + \omega_p \times (\omega_p \times \mathbf{R}_p)] + M\mathbf{R}_p \times \mathbf{g} - \mathbf{I}\alpha_p - \omega_p \times \mathbf{I}\omega_p \\
+\Re_p \mathbf{M}_{ext} + \sum_{i=1}^{6} \mathbf{f}_i + \sum_{i=1}^{6} \mathbf{q}_{\mathbf{p}_i} \times (\mathbf{Q}_{\mathbf{b}_i}\ddot{\mathbf{t}}_p - \mathbf{Q}_{\mathbf{b}_i}\tilde{\mathbf{q}}_{\mathbf{b}_i}\alpha_p) \\
-\sum_{i=1}^{6} \mathbf{q}_{\mathbf{p}_i} \times \{\mathbf{Q}_{\mathbf{p}_i}\ddot{\mathbf{t}}_p - \mathbf{Q}_{\mathbf{p}_i}\tilde{\mathbf{q}}_{\mathbf{p}_i}\alpha_p + \mathbf{V}_i - \mathbf{s}_i F_i\} &= \mathbf{0}. \quad (3.46)
\end{aligned}
$$

Again, substituting expressions of $\mathbf{a}$ and $(\mathbf{F}_s)_i$ from Eqns. (3.42) and (3.40) into Eqn. (3.46) and simplifying, we get

$$
\begin{aligned}
(M\tilde{\mathbf{R}}_p + \sum_{i=1}^{6} \tilde{\mathbf{q}}_{\mathbf{p}_i}\mathbf{Q}_{\mathbf{p}_i})\ddot{\mathbf{t}}_p - \sum_{i=1}^{6} \tilde{\mathbf{q}}_{\mathbf{p}_i}\mathbf{Q}_{\mathbf{b}_i}\ddot{\mathbf{t}}_p \\
+[\mathbf{I} + M(R_p^2\mathbf{E}_3 - \mathbf{R}_p\mathbf{R}_p^T) - \sum_{i=1}^{6} \tilde{\mathbf{q}}_{\mathbf{p}_i}\mathbf{Q}_{\mathbf{p}_i}\tilde{\mathbf{q}}_{\mathbf{p}_i}]\alpha_p \\
+\sum_{i=1}^{6} \tilde{\mathbf{q}}_{\mathbf{p}_i}\mathbf{Q}_{\mathbf{b}_i}\tilde{\mathbf{q}}_{\mathbf{b}_i}\alpha_p + \omega_p \times \mathbf{I}\omega_p \\
+M\mathbf{R}_p \times [(\omega_p \cdot \mathbf{R}_p)\omega_p - \mathbf{g}] + \sum_{i=1}^{6}(\mathbf{q}_{\mathbf{p}_i} \times \mathbf{V}_i - \mathbf{f}_i) &= \sum_{i=1}^{6}(\mathbf{q}_{\mathbf{p}_i} \times \mathbf{s}_i)F_i + \Re_p \mathbf{M}_{ext}. \quad (3.47)
\end{aligned}
$$

Combining Eqns. (3.45) and (3.47) we get the closed form dynamic equations as

$$
\mathbf{J}_p \begin{bmatrix} \ddot{\mathbf{t}}_p \\ \alpha_p \end{bmatrix} - \mathbf{J}_b \begin{bmatrix} \ddot{\mathbf{t}}_b \\ \alpha_b \end{bmatrix} + \eta = \mathbf{H}\mathbf{F} + \begin{bmatrix} \Re_p \mathbf{F}_{ext} \\ \Re_p \mathbf{M}_{ext} \end{bmatrix}, \quad (3.48)
$$

where

$$
\begin{aligned}
\mathbf{J}_p &= \mathbf{J}_{plat} + \sum_{i=1}^{6} \mathbf{J}_{p_i}, \\
\mathbf{J}_{plat} &= \begin{bmatrix} M\mathbf{E}_3 & -M\tilde{\mathbf{R}}_p \\ M\tilde{\mathbf{R}}_p & \mathbf{I} + M(R_p^2\mathbf{E}_3 - \mathbf{R}_p\mathbf{R}_p^T) \end{bmatrix}, \\
\mathbf{J}_{p_i} &= \begin{bmatrix} \mathbf{Q}_{\mathbf{p}_i} & -\mathbf{Q}_{\mathbf{p}_i}\tilde{\mathbf{q}}_{\mathbf{p}_i} \\ \mathbf{Q}_{\mathbf{p}_i}\tilde{\mathbf{q}}_{\mathbf{p}_i} & -\tilde{\mathbf{q}}_{\mathbf{p}_i}\mathbf{Q}_{\mathbf{p}_i}\tilde{\mathbf{q}}_{\mathbf{p}_i} \end{bmatrix}, \\
\mathbf{J}_b &= \sum_{i=1}^{6} \mathbf{J}_{\mathbf{b}i}, \\
\mathbf{J}_{b_i} &= \begin{bmatrix} \mathbf{Q}_{\mathbf{b}_i} & -\mathbf{Q}_{\mathbf{b}_i}\tilde{\mathbf{q}}_{\mathbf{b}_i} \\ \tilde{\mathbf{q}}_{\mathbf{p}_i}\mathbf{Q}_{\mathbf{b}_i} & -\tilde{\mathbf{q}}_{\mathbf{p}_i}\mathbf{Q}_{\mathbf{b}_i}\tilde{\mathbf{q}}_{\mathbf{b}_i} \end{bmatrix},
\end{aligned}
$$

$$
\begin{aligned}
\eta &= \eta_{plat} + \sum_{i=1}^{6} \eta_i, \\
\eta_{plat} &= \begin{bmatrix} M\{\omega_p \times (\omega_p \times \mathbf{R}_p) - \mathbf{g}\} \\ \omega_p \times \mathbf{I}\omega_p + M\mathbf{R}_p \times \{(\omega_p \cdot \mathbf{R}_p)\omega_p - \mathbf{g}\} \end{bmatrix}, \\
\eta_i &= \begin{bmatrix} \mathbf{V}_i \\ \mathbf{q_{p_i}} \times \mathbf{V}_i - \mathbf{f}_i \end{bmatrix}, \\
\mathbf{H} &= \begin{bmatrix} \mathbf{s_1} & \mathbf{s_2} & \mathbf{s_3} & \mathbf{s_4} & \mathbf{s_5} & \mathbf{s_6} \\ \mathbf{q_{p_1}} \times \mathbf{s_1} & \mathbf{q_{p_2}} \times \mathbf{s_2} & \mathbf{q_{p_3}} \times \mathbf{s_3} & \mathbf{q_{p_4}} \times \mathbf{s_4} & \mathbf{q_{p_5}} \times \mathbf{s_5} & \mathbf{q_{p_6}} \times \mathbf{s_6} \end{bmatrix}, \text{and} \\
\mathbf{F} &= [F_1 \quad F_2 \quad F_3 \quad F_4 \quad F_5 \quad F_6]^T.
\end{aligned}
$$

The forces, coming from the base platform and exerted by the actuators, will be transmitted to the top platform through the legs only. As the legs are flexible, there is a small relative acceleration between any two points in the legs. Hence an inertia force also comes due to it. But for a Stewart platform, constructed for practical application (for vibration isolation, tracking, sensor application, etc.), the stiffness of the legs are enough to make this inertia force negligibly small. Therefore, the net force transmitted to the top platform through a leg is equal to the force generated due to the deformation of the legs. So, for i-th leg,

$$F_i = (K_{leg})_i(L_{0i} - L_i)$$

where

$$
\begin{aligned}
L_{0i} &= \text{equilibrium length of } i\text{-th leg.} \\
L_i &= \text{current length of } i\text{-th leg.}
\end{aligned}
$$

3.3 Conclusions

Using the Newton-Euler approach, the dynamic formulation of a 6-UPS Stewart platform has been carried out in the previous section. This model can be used for design and control purposes. For designing a Stewart platform some forces and moments, the expressions of which have not been given so far, are also necessary to be calculated to find the strength and deflection of the structure. Those can be easily found out from the forces and accelerations, already determined.

Here we have assumed lumped stiffness of the legs and neglected the inertia forces, coming on the legs due to their flexibility. Using *finite element* and *finite difference* method these

restrictions can be avoided. But the finite element models, being too computation intensive, would make simulations very slow. This hindrance also can be circumvented by exploiting the inherent parallel nature of the Stewart platform . The calculations for *six* legs can be done independent of each other, only with the information of base and top platform motions. Owing to this fact, use of parallel programing will drastically reduce the computational time. These can be explored in a future work in this area.

Chapter 4

Validation of Linearized Model

4.1 Introduction

In chapter 2, we have used the *lowest natural frequency* as a measure of stability of a manipulator. Calculation of natural frequencies from the linearized dynamic model was explained by taking 6-UPS Stewart platform as an example. In this chapter with the help of numerical simulations we have justified that linearization.

4.2 Numerical Simulations

The dynamics of Stewart platform is expressed by a *system of stiff, coupled, nonlinear, second order, ordinary differential equations* [34, 18]. Till now, no analytical solution of these kind of equations has been found out. Taking *position, orientation, linear and angular velocities* as state variables, we express Eqn. (3.48) in *state-space* as

$$\dot{\mathbf{z}} = \begin{bmatrix} \mathbf{z}(7:12) \\ \mathbf{J}_p^{-1}\left(\mathbf{HF} + \begin{bmatrix} \Re_p \mathbf{F}_{ext} \\ \Re_p \mathbf{M}_{ext} \end{bmatrix} - \eta + \mathbf{J}_b \begin{bmatrix} \ddot{\mathbf{t}}_b \\ \alpha_b \end{bmatrix}\right) \end{bmatrix}. \tag{4.1}$$

Here $\mathbf{z}$ is the state vector, and is given by

$$\mathbf{z} = \begin{bmatrix} t_{p_x} & t_{p_y} & t_{p_z} & \theta_{p_x} & \theta_{p_y} & \theta_{p_z} & \dot{t}_{p_x} & \dot{t}_{p_y} & \dot{t}_{p_z} & \omega_{p_x} & \omega_{p_y} & \omega_{p_z} \end{bmatrix}^T. \tag{4.2}$$

Numerical solution of Eqn. (4.1) have been performed in MATLAB for the test manipulator II, given in appendix A, for the top platform's reference position, $(0, 0, 0.085)$ and orientation, $(0, 0, 0)$, subjected to base excitations at different frequencies. We get two distinct nature of responses of the top platform, depending on whether the excitation frequencies are equal to

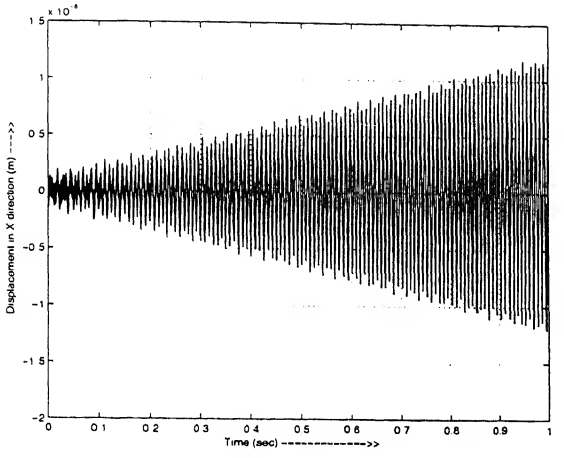

Translation in X direction

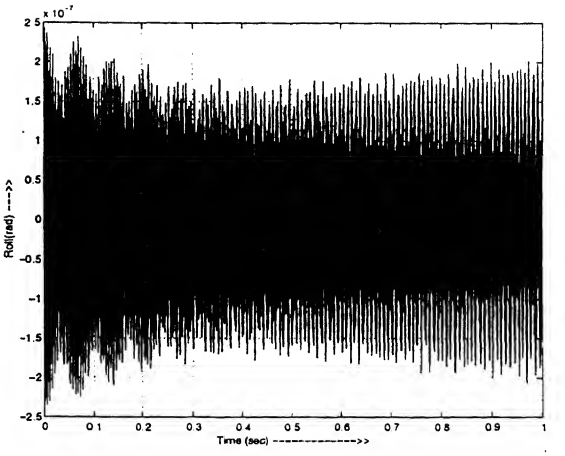

Rotation about X axis

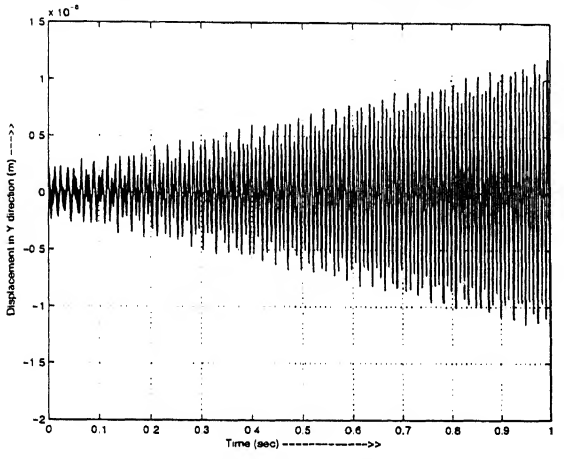

Translation in Y direction

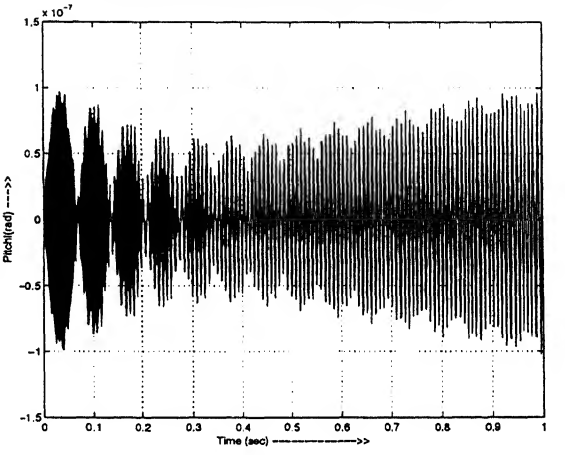

Rotation about Y axis

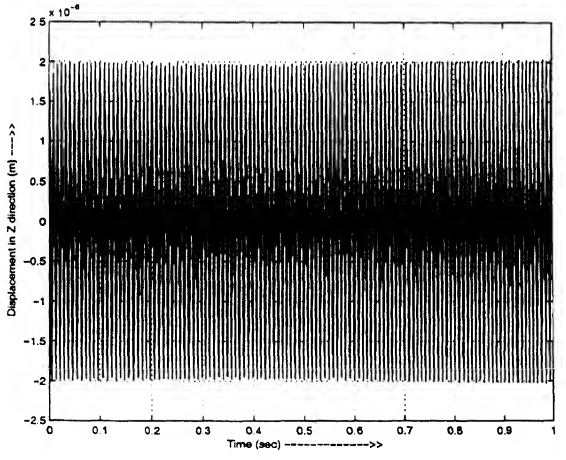

Translation in Z direction

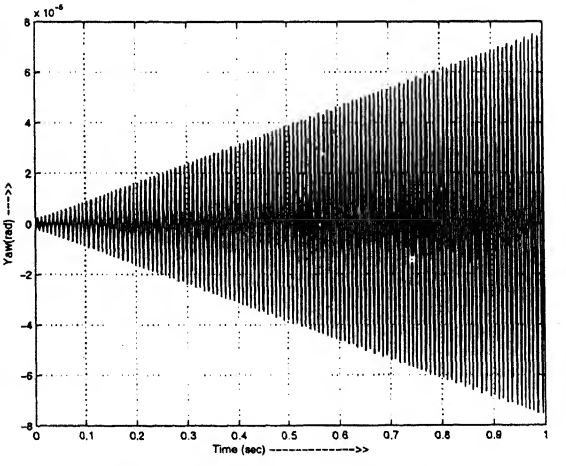

Rotation about Z axis

Figure 4.1: Displacement from Equilibrium Position Vs Time Plot at Base Excitation Frequency Equal to 2nd Natural Frequency, $\omega = 749.715$ Hz

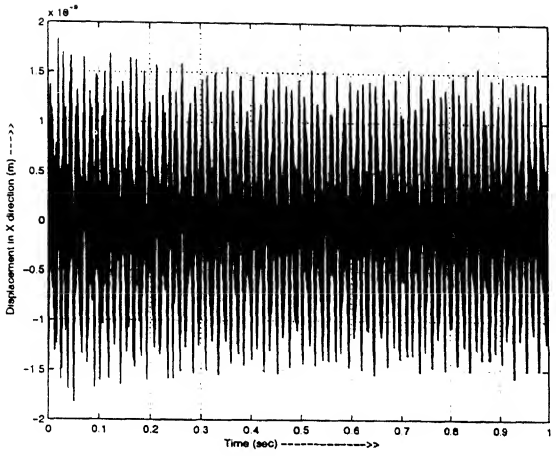

Translation in X direction

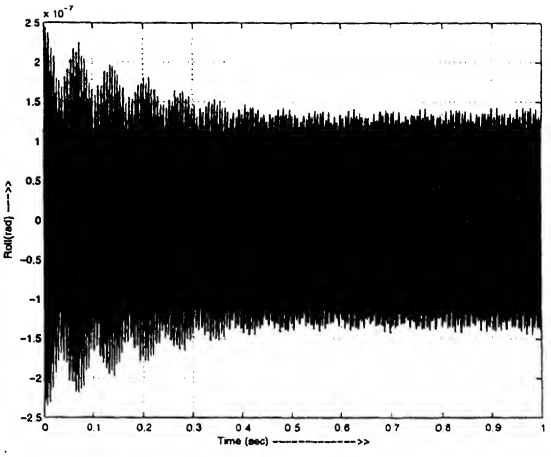

Rotation about X axis

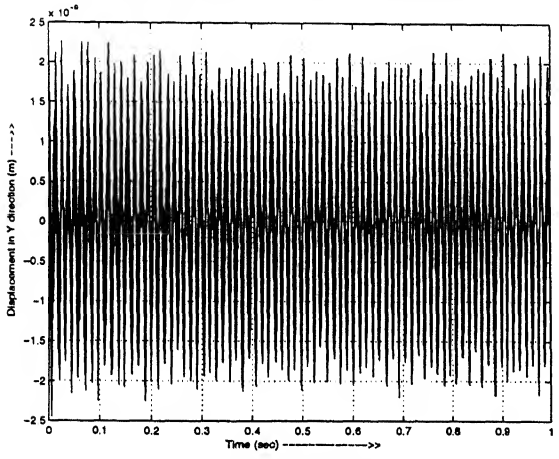

Translation in Y direction

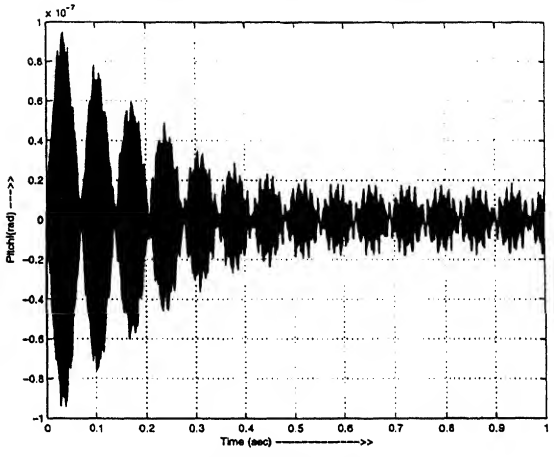

Rotation about Y axis

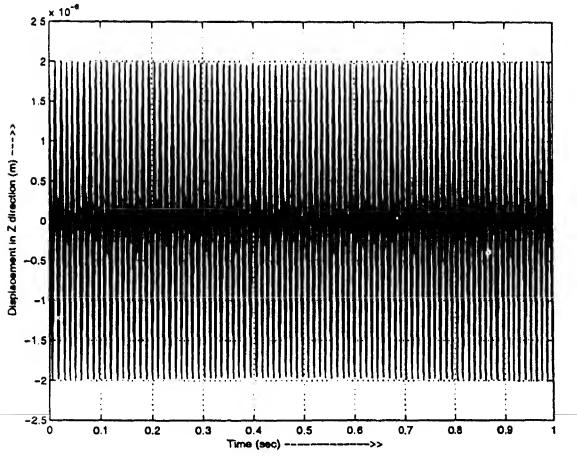

Translation in Z direction

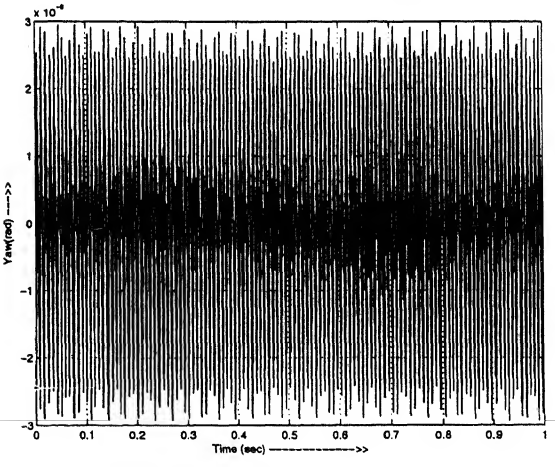

Rotation about Z axis

Figure 4.2: Displacement from Equilibrium Position Vs Time Plot at Base Excitation Frequency, $\omega = 550.136$, Away from Natural Frequencies

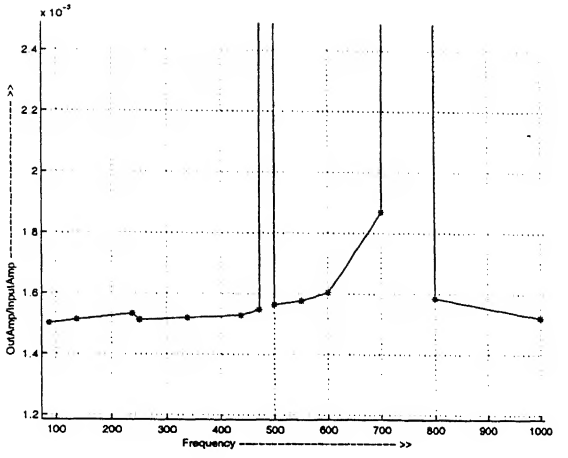

Translation in X direction

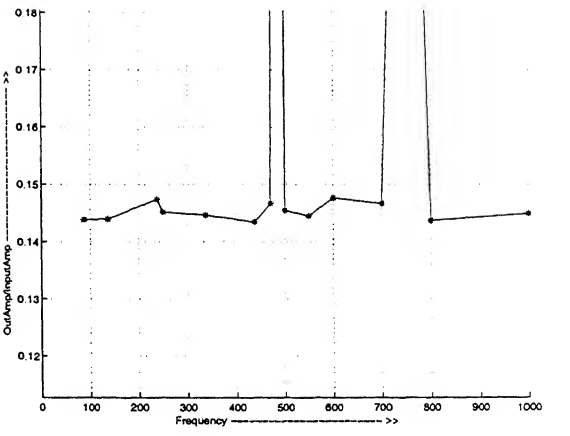

Rotation about X axis

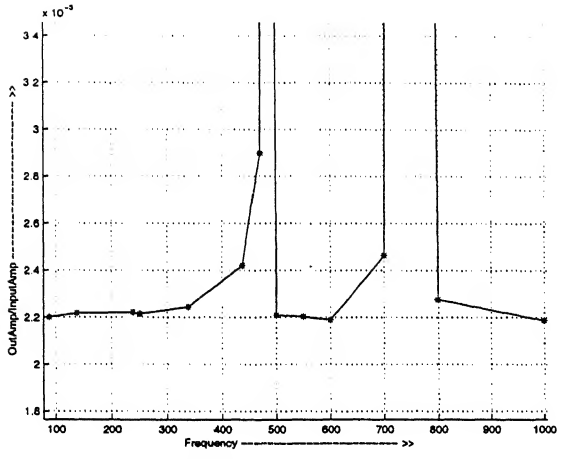

Translation in Y direction

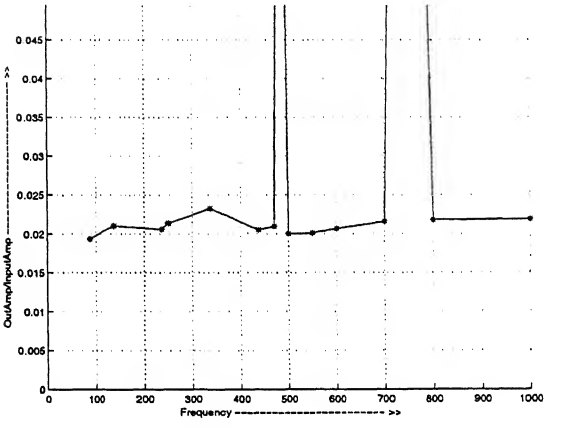

Rotation about Y axis

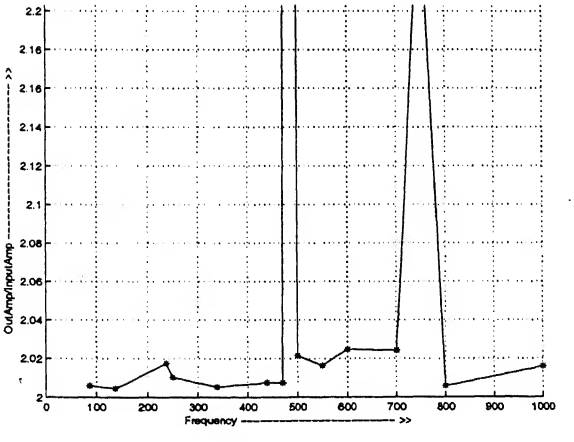

Translation in Z direction

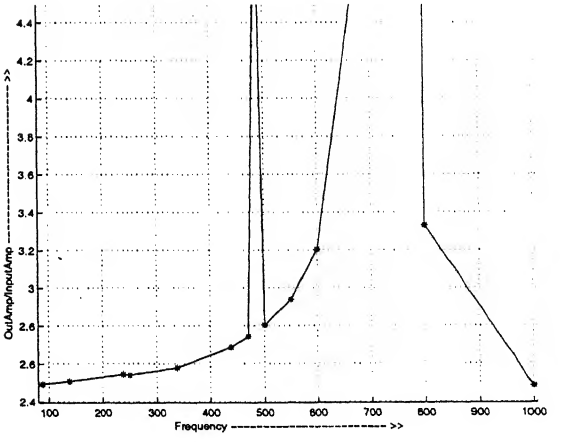

Rotation about Z axis

Figure 4.3: Vibration Amplitude and Excitation Amplitude Ratio Vs Excitation Frequency

the natural frequencies or away from it. Two typical plots one at the 2nd natural frequency (Fig. 4.1) and other at away from the natural frequencies (Fig. 4.2) have been shown.

For different base excitation frequencies, we get the results shown in Fig. (4.1) and Fig. (4.2), depending upon whether the frequency matches with the natural frequencies or not. For different base excitations if we plot the ratio of the response amplitude to the base excitation amplitude against the base excitation frequency, we get a plot like Fig. (4.3). From the dynamic model, it is clear that the Stewart platform has *six* natural frequencies. (With flexible legs the platform actually it has infinite number of natural frequencies, due to approximations it comes to *six*.) Computations have been carried out for base excitation frequency up to a little above the second natural frequency.

4.3 Conclusions

It is clear from Figs: (4.1) and (4.3) that the Stewart platform exhibits resonance at the natural frequencies, calculated from the linearized dynamic model. Hence these frequencies can be considered as a representative of the system dynamics. If the lowest natural frequency is very small the manipulator tends to be unstable and fails to support loads or to track a trajectory.

Chapter 5

Vibration Control

5.1 Introduction

Originally, the Stewart platform was developed for flight simulations. But, soon, it found its use in several applications, due to its *six*-DOF motion capabilities. High load carrying capacities and precise positioning capabilities give it a wide range of applicability from supporting missile launch pad to micro-scale sensor applications. One of the application is as a vibration isolator. From literature review we see, though many types of controllers have been designed assuming rigid body model of the Stewart platform, its flexibility is not taken into account.

In this chapter, a proportional plus derivative (PD) control strategy for isolating any device, mounted on a Stewart platform, from surrounding vibrations has been elaborated, considering the flexibility of the legs. For calculation of gains, a linearized model of the Stewart platform is developed. Then, using the PD controller, numerical simulations of free and forced vibration control have been performed to evaluate the system performance.

5.2 Vibration Control Strategy

We have used PD control in *task space*. We can get the displacements and velocities of the reference point of the top platform in task space in following ways.

- We can directly measure the displacement of the platform reference point by camera sensor and get its velocity by using numerical differentiation [31, 18]. In this case, central difference scheme will be preferable.

- We can obtain the acceleration of the platform reference point by accelerometer and get

displacement and velocity by numerical integration [31].

- We can measure the change of leg-length and its rate by means of instrumentation of the active joints. From that, we can solve the forward kinematics to find out displacement and velocity of the platform reference point in task space. (In general forward kinematics of parallel manipulators requires solution of a set of coupled nonlinear algebraic equations which is computation intensive. But, as the next point is always very close to the previous point so Newton-Raphson or other local methods [31] will very quickly converge if the previous point is taken as an initial guess for the numerical routines. Only for the initial point it will take considerable time.)

- Any combination of the above methods.

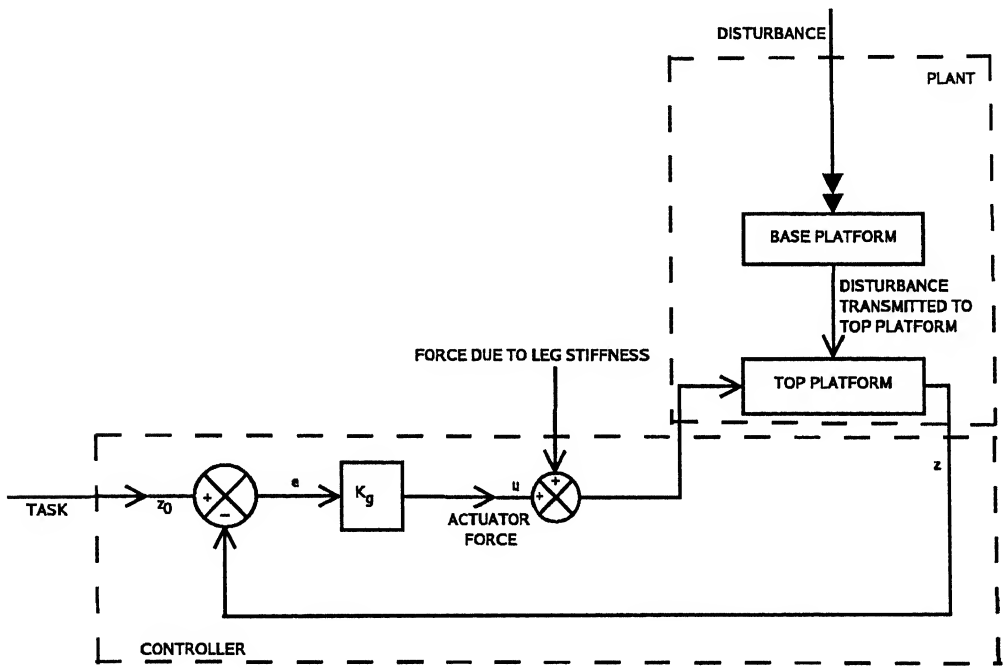

Figure 5.1: Control Diagram

If there were *six* actuators which could apply Cartesian forces directly on the top platform to stabilize its motion, let $\overline{\mathbf{u}}$ be the force vector applied by them. Here $\overline{\mathbf{u}}$ is a 6×1 vector and each component of it signifies the force given by each of those virtual actuators. Then the dynamic Eqn. (3.48) becomes

$$\mathbf{J}_p \begin{bmatrix} \ddot{\mathbf{t}}_p \\ \alpha_p \end{bmatrix} - \mathbf{J}_b \begin{bmatrix} \ddot{\mathbf{t}}_b \\ \alpha_b \end{bmatrix} + \eta \;=\; \mathbf{HF} + \begin{bmatrix} \Re_p \mathbf{F}_{ext} \\ \Re_p \mathbf{M}_{ext} \end{bmatrix} + \overline{\mathbf{u}}. \tag{5.1}$$

Let the force vector $\overline{\mathbf{u}}$ be generated by a virtual PD controller having gains $\overline{\mathbf{K}}_g$. If $\delta\mathbf{z}$ is the perturbation of the state vector from its equilibrium position $\mathbf{z}_0$, then the force generated by the actuator is

$$\overline{\mathbf{u}} = -\overline{\mathbf{K}}_g \delta\mathbf{z} \tag{5.2}$$

where

$$\delta\mathbf{z} = \mathbf{z}(t) - \mathbf{z}(0) = \mathbf{z}(t) - \mathbf{z}_0$$

The gain matrix is partitioned into two parts: proportional gains, $\overline{\mathbf{K}}_p$ and velocity gains, $\overline{\mathbf{K}}_v$. Therefore

$$\overline{\mathbf{K}}_g = [\overline{\mathbf{K}}_p \;\; \overline{\mathbf{K}}_v]. \tag{5.3}$$

Eqn. (5.1) can be written in state space as

$$\dot{\mathbf{z}} = \begin{bmatrix} \mathbf{z}(7:12) \\ \mathbf{J}_p^{-1}\left(\mathbf{HF} + \begin{bmatrix} \Re_p \mathbf{F}_{ext} \\ \Re_p \mathbf{M}_{ext} \end{bmatrix} - \eta + \mathbf{J}_b \begin{bmatrix} \ddot{\mathbf{t}}_b \\ \alpha_b \end{bmatrix}\right) \end{bmatrix} + \begin{bmatrix} \mathbf{0} \\ \mathbf{J}_p^{-1}\overline{\mathbf{u}} \end{bmatrix}. \tag{5.4}$$

Here, $\mathbf{J}_b \begin{bmatrix} \ddot{\mathbf{t}}_b \\ \alpha_b \end{bmatrix}$ is not known a priori. But depending on the applications, a rough estimation of the maximum magnitudes of $\ddot{\mathbf{t}}_b$ and α_b can be made. At the desired control position, we know the value of $\mathbf{J}_b$. Hence a preliminary approximation of the whole term can be made, and denoted as $\mathbf{d}$.

The first term of the right hand side of Eqn. (5.4) can be expanded in Taylor's series around equilibrium point ($\mathbf{z}_0$) as following manner

$$\text{First term} = f(\mathbf{z}_0) + \mathbf{A}\delta\mathbf{z} + \text{Higher order terms} \tag{5.5}$$

where

$$\mathbf{A} = \text{Jacobian of} \begin{bmatrix} \mathbf{z}(7:12) \\ \mathbf{J}_p^{-1}\left(\mathbf{HF} + \begin{bmatrix} \Re_p \mathbf{F}_{ext} \\ \Re_p \mathbf{M}_{ext} \end{bmatrix} - \eta + \mathbf{d}\right) \end{bmatrix}.$$

The expression of Jacobian is developed in the appendix B.

As $\mathbf{z}_0$ is the equilibrium point,

$$f(\mathbf{z}_0) = \mathbf{0}. \tag{5.6}$$

Using Eqn. (5.2), the second term of Eqn. (5.4) can be written as

$$\begin{bmatrix} \mathbf{0} \\ \mathbf{J}_p^{-1}\overline{\mathbf{u}} \end{bmatrix} = \begin{bmatrix} \mathbf{0} \\ \mathbf{J}_p^{-1} \end{bmatrix} \overline{\mathbf{u}} = - \begin{bmatrix} \mathbf{0} \\ \mathbf{J}_p^{-1} \end{bmatrix} \overline{\mathbf{K}}_g \delta \mathbf{z} = -\mathbf{B}\overline{\mathbf{K}}_g \delta \mathbf{z} \tag{5.7}$$

where

$$\mathbf{B} = \begin{bmatrix} \mathbf{0} \\ \mathbf{J}_p^{-1} \end{bmatrix}.$$

From Eqn. (5.5), Eqn. (5.6) and Eqn. (5.7), we can write Eqn. (5.4) up to first order approximation as

$$\dot{\mathbf{z}}(t) = (\mathbf{A} - \mathbf{B}\overline{\mathbf{K}}_g)\delta \mathbf{z}(t). \tag{5.8}$$

Hence for no steady state error the eigen values of $(\mathbf{A} - \mathbf{B}\overline{\mathbf{K}}_g)$ have to be on the left half of s-plane. Now by any standard pole placement method we can get $\overline{\mathbf{K}}_g$. (Refer Ogata [30], for a detailed discussion on pole placement methods.)

The gains evaluated above would have stabilized the platform if the controlling forces instead of through legs were applied directly on the top platform by actuators. Hence if the force transformation matrix at the desired position is $\mathbf{H}_0$, the actual gains are,

$$\mathbf{K}_g = \mathbf{H}_0^{-1}\overline{\mathbf{K}}_g. \tag{5.9}$$

Now $\mathbf{K}_g$ consist of actual proportional and derivative gains

$$\mathbf{K}_g = [\mathbf{K}_p \;\; \mathbf{K}_v]. \tag{5.10}$$

The control force generated by the actuators at the legs are

$$\mathbf{u} = -\mathbf{K}_g \delta \mathbf{z}. \tag{5.11}$$

As this control force, $\mathbf{u}$ is applied through leg actuators, they will also compress the legs and will be a part of leg force $\mathbf{F}$ along with the spring force generated due to base motions.

5.3 Simulations

Using the vibration control strategy, described in the previous section, numerical simulations of control of *actual plant* against *free vibrations* and *vibration due to base motions* have been made. Some of the results are presented in the next two sections.

5.3.1 Free Vibration Control

For the simulation of free vibration, a small instantaneous displacement of the top platform has been given in absence of any other external disturbances. Numerical data of the platforms, given in the appendix A, have been used for simulations.

All numerical values are in SI units. As the positions and velocities of the Stewart platform are strongly coupled, hence, general gain matrices have been used for controlling the vibration instead of diagonal gain matrices. These coupled gain matrices improve the controller performance.

1. **Case 1: Test manipulator I**

$$\begin{aligned} \text{Desired position:} \quad & [-0.15 \quad -0.05 \quad 0.39]^T, \text{ and} \\ \text{orientation:} \quad & [0.4 \quad 0.2 \quad 0]^T. \\ \text{Disturbed position:} \quad & [-0.1499533 \quad -0.050002 \quad 0.390070]^T, \text{ and} \\ \text{orientation:} \quad & [0.399733 \quad 0.199992 \quad 3.579856]^T. \end{aligned}$$

The positions of the poles in s-plane are shown in Fig. (5.2). Proportional and derivative gain matrices are given below.

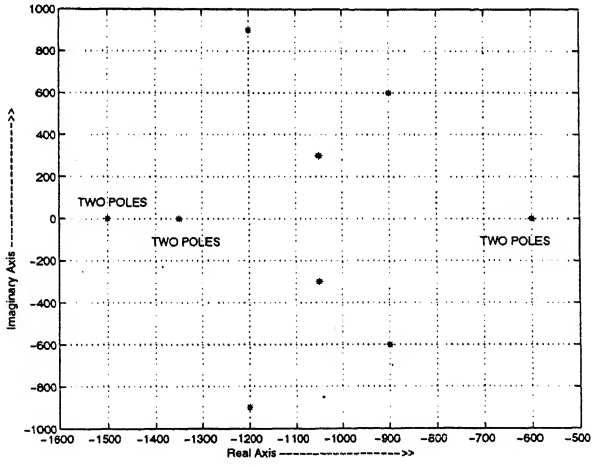

Figure 5.2: Pole Positions in s-plane for Free Vibration Control of Test Manipulator I

$$\mathbf{K}_p = 10^6 \times \begin{bmatrix} 619.991 & 1311.487 & 1598.334 & -101.713 & -1475.722 & 885.982 \\ -22.659 & -883.634 & -1573.340 & -0.690 & 1258.533 & -888.109 \\ -220.618 & 208.040 & 561.084 & -47.985 & -443.240 & 395.926 \\ 207.997 & 595.413 & -139.676 & -21.783 & -389.184 & 105.009 \\ 1616.698 & -298.718 & 737.603 & -199.752 & -304.517 & -66.533 \\ -2214.663 & -828.419 & -2041.813 & 317.959 & 1404.277 & -422.330 \end{bmatrix}$$

$$\mathbf{K}_v = 10^3 \times \begin{bmatrix} 862.525 & 140.704 & 318.976 & -193.860 & -156.365 & 677.732 \\ 3.653 & -1154.190 & -2656.574 & 80.863 & 1264.901 & -710.163 \\ -251.774 & -36.448 & 1484.511 & 18.353 & -469.573 & 401.079 \\ 333.842 & 1318.403 & -298.774 & 4.062 & -348.514 & -68.029 \\ 2556.786 & -755.532 & 1861.394 & -400.705 & -160.399 & -112.436 \\ -4215.574 & -706.665 & -3807.508 & 598.105 & 1303.164 & -146.496 \end{bmatrix}$$

The control plots are presented in Fig. (5.3).

2. **Case 2: Test manipulator II**

Desired position: $[0 \quad 0 \quad 0.085]^T$, and

orientation: $[0 \quad 0 \quad 0]^T$.

Disturbed position: $[-1.95 \times 10^{-5} \quad 6.164 \times 10^{-5} \quad 0.0849996]^T$, and

orientation: $[284.762 \times 10^{-6} \quad 164.378 \times 10^{-6} \quad 2.017 \times 10^{-6}]^T$.

The positions of the poles in s-plane are shown in the Fig. (5.4). Proportional and derivative gain matrices are given below.

$$\mathbf{K}_p = 10^5 \times \begin{bmatrix} -946.586 & 1851.341 & -329.509 & -440.342 & -261.999 & 2663.938 \\ 1145.126 & -1376.650 & -1029.038 & 271.152 & 227.342 & -1814.607 \\ -726.601 & -1934.165 & -1097.727 & 359.141 & 243.555 & -2356.249 \\ 353.132 & 2056.321 & -310.414 & -474.549 & -363.133 & 2856.158 \\ 1669.7535 & 133.309 & -726.146 & 24.127 & 1.372 & 55.613 \\ -1493.797 & -656.915 & -935.943 & 228.617 & 128.284 & -1195.752 \end{bmatrix}$$

$$\mathbf{K}_v = 10^2 \times \begin{bmatrix} -875.909 & 1893.424 & 197.206 & -136.271 & -279.742 & 1177.966 \\ 147.533 & -1315.242 & -85.325 & 93.972 & 192.657 & -815.661 \\ -946.363 & -1835.209 & -33.377 & 122.547 & 249.190 & -998.750 \\ 228.969 & 2177.518 & 129.951 & -147.610 & -306.197 & 1223.562 \\ 1818.630 & -43.312 & 79.275 & -4.164 & 5.018 & 46.792 \\ -1699.681 & -849.858 & -58.471 & 62.857 & 115.339 & -543.643 \end{bmatrix}$$

The control plots are presented in Fig. (5.5).

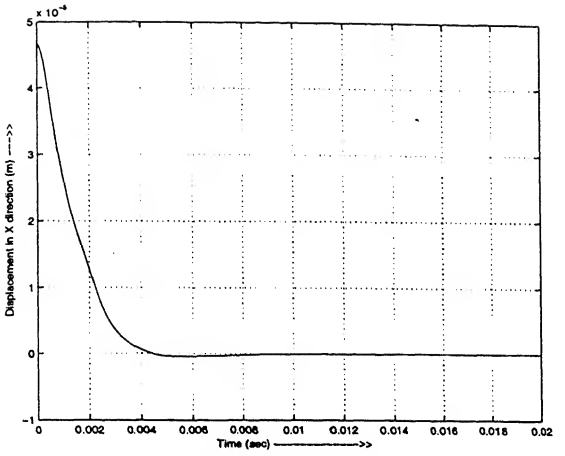

Translation in X direction

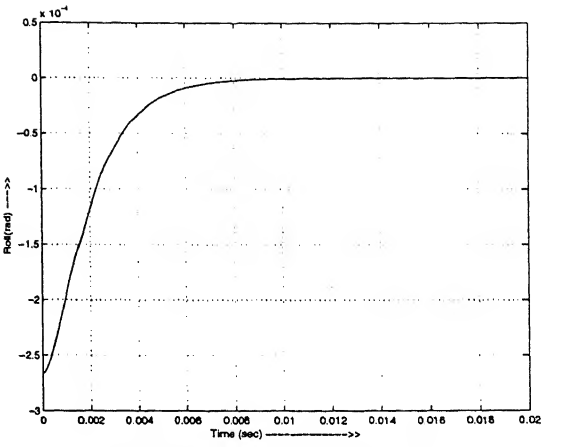

Rotation about X axis

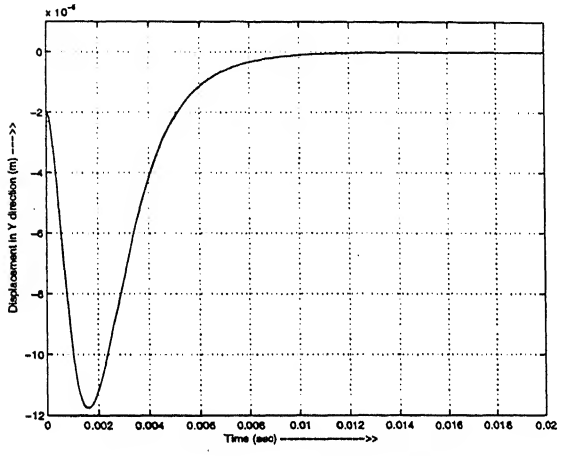

Translation in Y direction

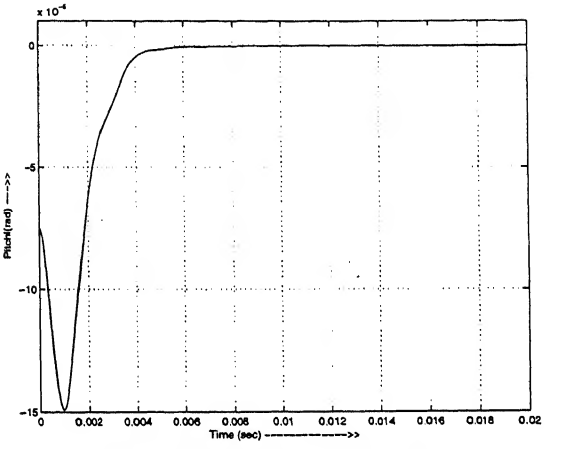

Rotation about Y axis

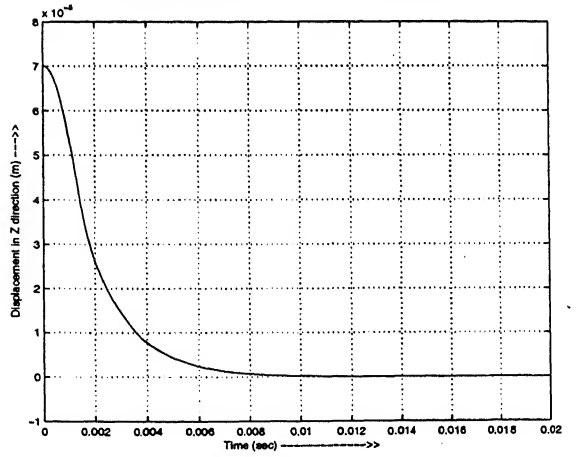

Translation in Z direction

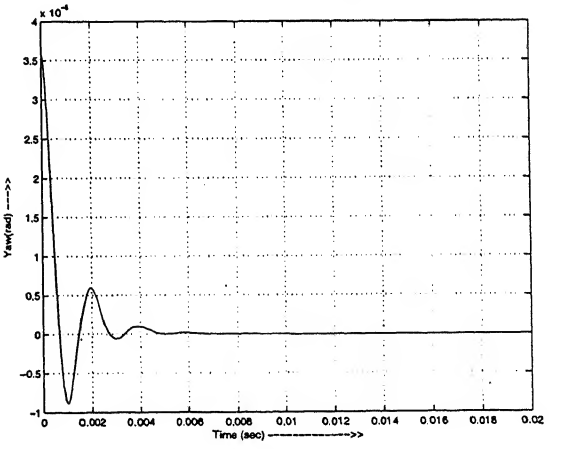

Rotation about Z axis

Figure 5.3: Free Vibration Control of Test Manipulator I

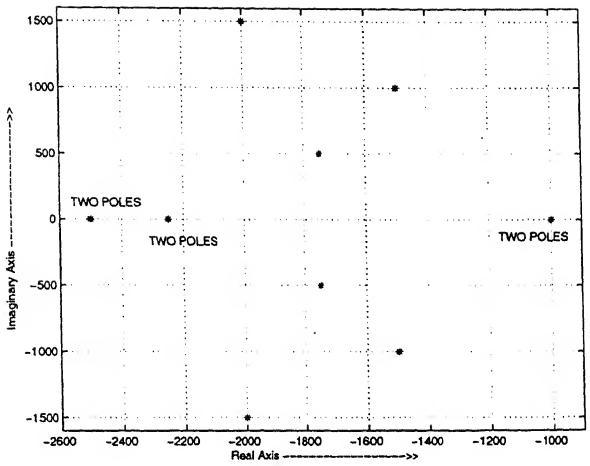

Figure 5.4: Pole Positions in s-plane for Free Vibration Control of Test Manipulator II

5.3.2 Control of Vibration due to Base Motion

In this section, simulations of vibration control of the top platform from the base motions have been done. For the reason described in the previous section, general gain matrices have been used for controlling the top platform motion. Here also, all values are in SI units.

1. **Case 1: Test manipulator I**

$$\begin{aligned} \text{Desired position:} \quad & [-0.15 \quad -0.05 \quad 0.39]^T, \text{ and} \\ \text{orientation:} \quad & [0.4 \quad 0.2 \quad 0]^T. \end{aligned}$$

Base has *six* degrees of motion. Motion is assumed to be sinusoidal. In X, Y and Z direction the frequency is 15 Hz and amplitude is 0.001 m. For Roll, Pitch and Yaw the frequency is 10 Hz and amplitude is 0.0001 rad.

The positions of the poles in s-plane are shown in Fig. (5.6). Proportional and derivative gain matrices are given below.

$$\mathbf{K}_p = 10^8 \times \begin{bmatrix} 491.093 & 1472.985 & 1329.266 & -284.528 & -1026.719 & 840.444 \\ 1.827 & -1.238.164 & -1.108.064 & 191.276 & 792.576 & -794.389 \\ -143.748 & 231.715 & 627.870 & -24.983 & -175.760 & 306.262 \\ 189.758 & 847.762 & -147.649 & -94.791 & -448.436 & 214.406 \\ 1453.537 & -252.967 & 819.228 & -201.008 & -10.926 & -194.647 \\ -2392.052 & -1038.071 & -1628.026 & 466.697 & 890.805 & -333.970 \end{bmatrix}$$

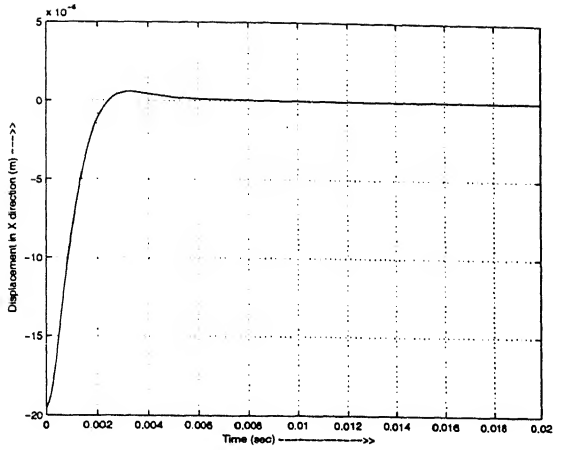

Translation in X direction

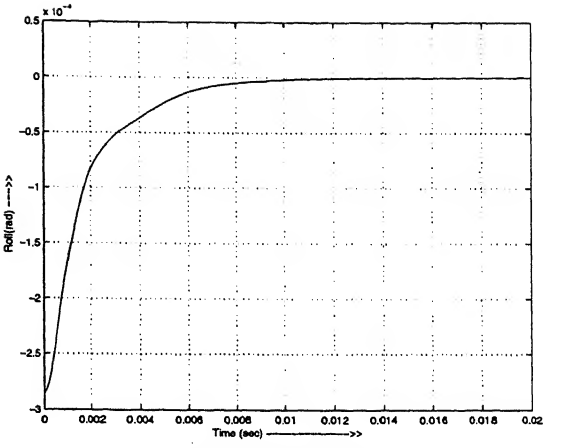

Rotation about X axis

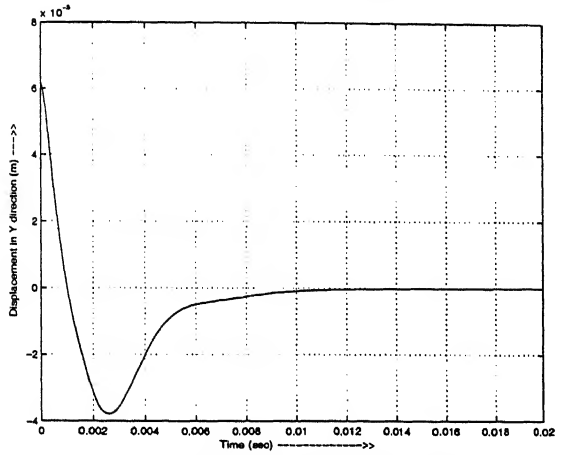

Translation in Y direction

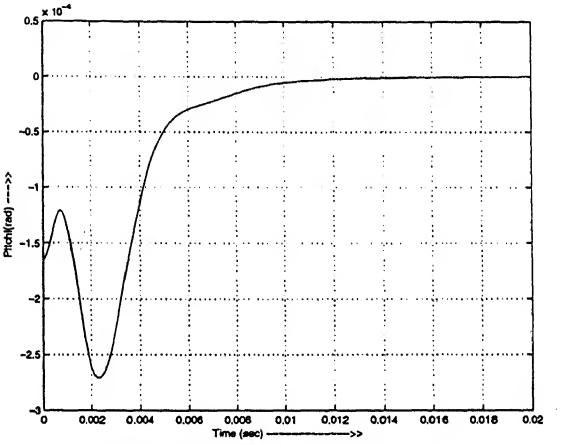

Rotation about Y axis

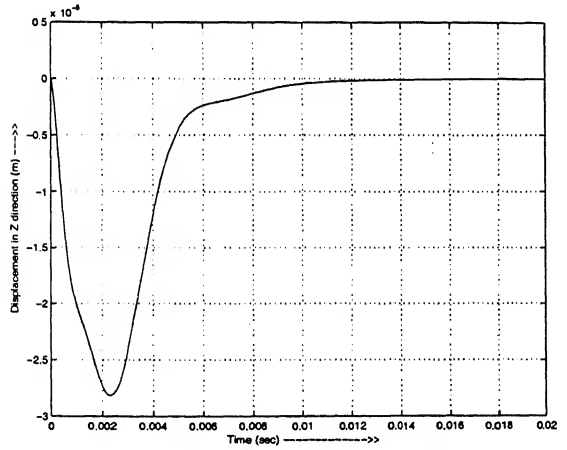

Translation in Z direction

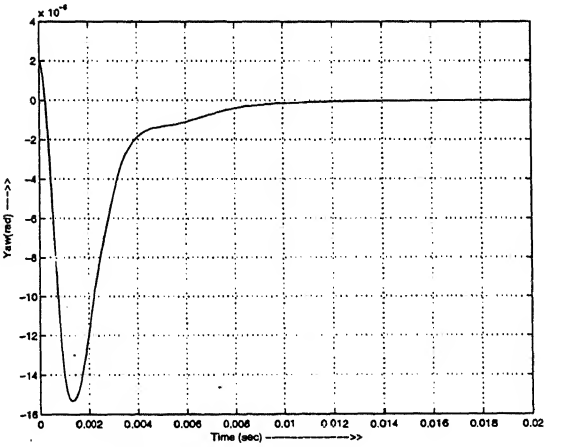

Rotation about Z axis

Figure 5.5: Free Vibration Control of Test Manipulator II

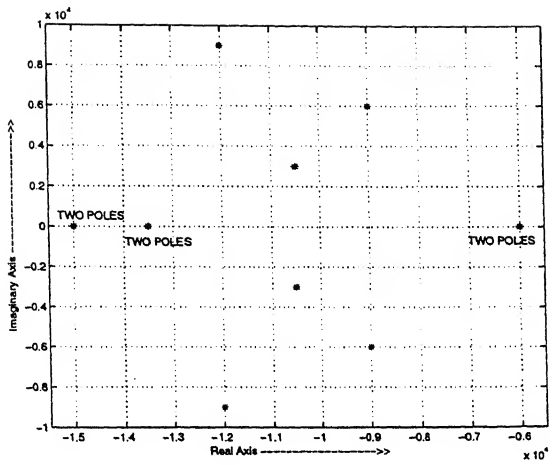

Figure 5.6: Pole Positions in s-plane for Controlling Vibrations Due to Base Motions (Test Manipulator I)

$$\mathbf{K}_p = 10^5 \times \begin{bmatrix} 86.252 & 167.020 & 290.316 & -31.781 & -119.779 & 68.196 \\ 0.365 & -137.375 & -240.525 & 18.557 & 94.679 & -71.371 \\ -25.177 & 6.353 & 140.306 & -0.304 & -26.632 & 38.282 \\ 33.384 & 134.250 & -40.004 & -6.283 & -42.716 & -2.735 \\ 255.678 & -65.888 & 185.377 & -39.345 & 4.996 & -15.752 \\ -421.557 & -98.311 & -358.182 & 69.871 & 90.135 & -12.013 \end{bmatrix}$$

The control plots are presented in Fig. (5.7).

2. **Case 2: Test manipulator II**

$$\begin{aligned} \text{Desired position:} \quad & [0 \quad 0 \quad 0.085]^T, \text{ and} \\ \text{orientation:} \quad & [0 \quad 0 \quad 0]^T. \end{aligned}$$

The gains are calculated based only on the information that the base platform will be subjected to maximum positional disturbance of 0.01 m. No assumption has been made regarding nature of the excitation or the magnitude of velocity and acceleration of the base due to disturbances.

The positions of the poles in s-plane are shown in Fig. (5.8). Proportional and derivative gain matrices are given below.

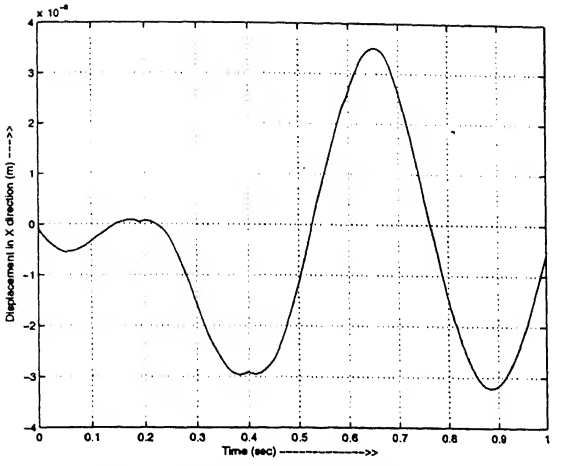

Translation in X direction

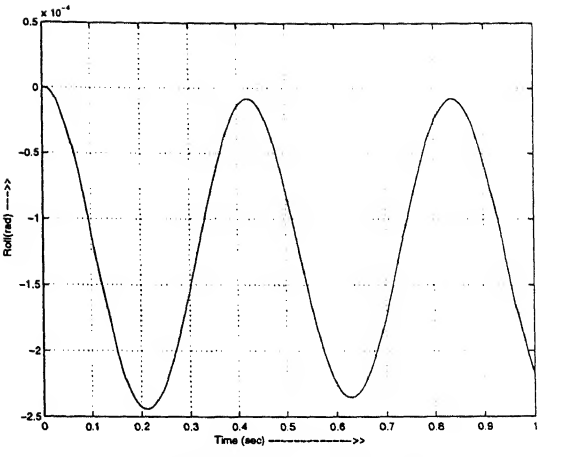

Rotation about X axis

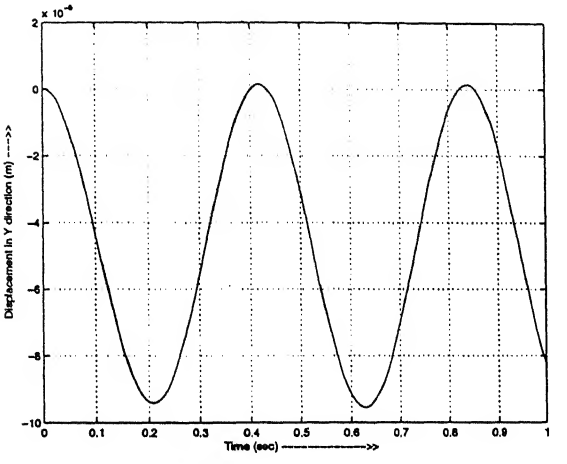

Translation in Y direction

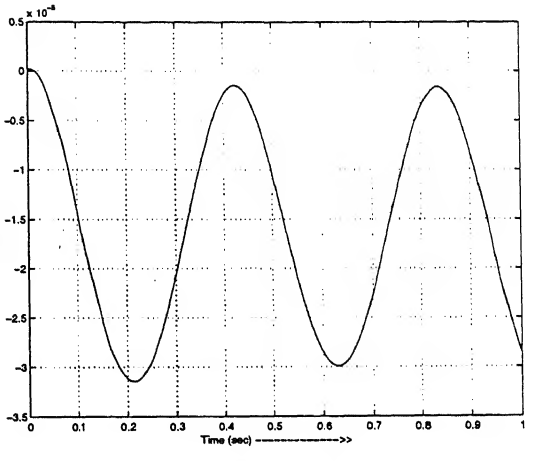

Rotation about Y axis

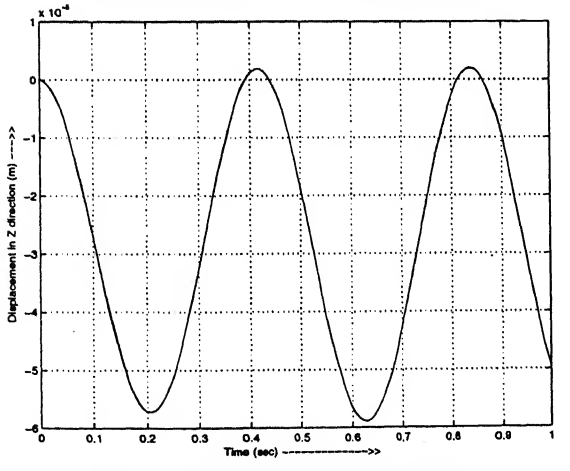

Translation in Z direction

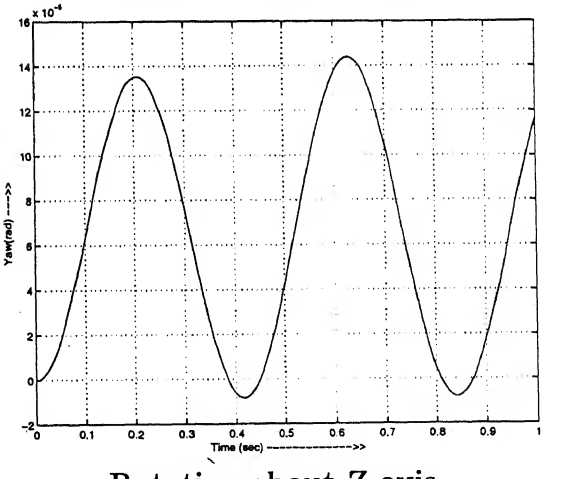

Rotation about Z axis

Figure 5.7: Control of Vibration Due to Base Excitation (Test Manipulator I)

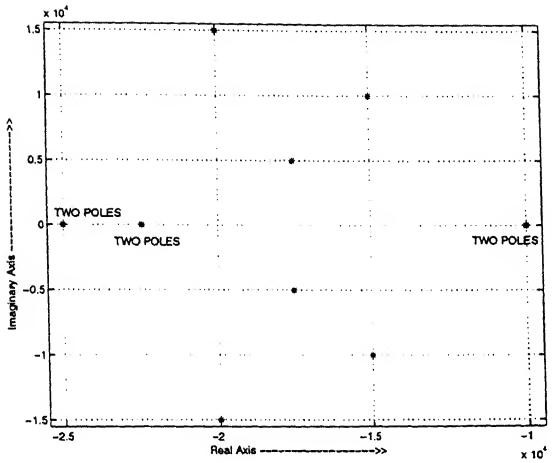

Figure 5.8: Pole Positions in s-plane for Controlling Vibrations Due to Base Motions of Test Manipulator I

$$\mathbf{K}_p = 10^7 \times \begin{bmatrix} -916.842 & 1343.907 & 648.639 & -1548.207 & -0.868.133 & 3356.666 \\ 1529.756 & -945.913 & -416.583 & 1058.049 & 596.751 & -2305.996 \\ -973.280 & -1338.406 & -489.040 & 1385.735 & 781.825 & -2.928.540 \\ 246.350 & 1578.074 & 653.746 & -1703.212 & -962.267 & 3.612.117 \\ 1886.245 & -35.652 & 64.239 & -37.787 & -3.754 & 112.993 \\ -1771.092 & -599.658 & -272.639 & 682.838 & 368.920 & -1494.026 \end{bmatrix}$$

$$\mathbf{K}_v = 10^4 \times \begin{bmatrix} -96.735 & 172.142 & 30.323 & -61.375 & -52.014 & 147.530 \\ 161.927 & -121.548 & -15.324 & 41.975 & 35.864 & -102.282 \\ -103.035 & -169.928 & -10.453 & 55.345 & 46.110 & -124.011 \\ 25.870 & 200.549 & 23.003 & -67.823 & -56.944 & 153.461 \\ 199.361 & -4.328 & 9.463 & -1.449 & -0.108 & 7.262 \\ -187.268 & -77.528 & -10.251 & 27.052 & 21.761 & -67.074 \end{bmatrix}$$

The base platform is subjected to random excitation in z-direction as shown in Fig. (5.9).

The controlled response of the top platform is presented in Fig. (5.10). Some portion of Fig. (5.10) is zoomed in Fig. (5.11) to show the response of the top platform clearly.

5.4 Conclusion

The simulations shows that even though no particular nature of the disturbances are assumed, the control strategy, developed here, worked quite well. Gains, calculated from the linearized dynamic model, should be increased a little at the time of simulating or controlling the actual

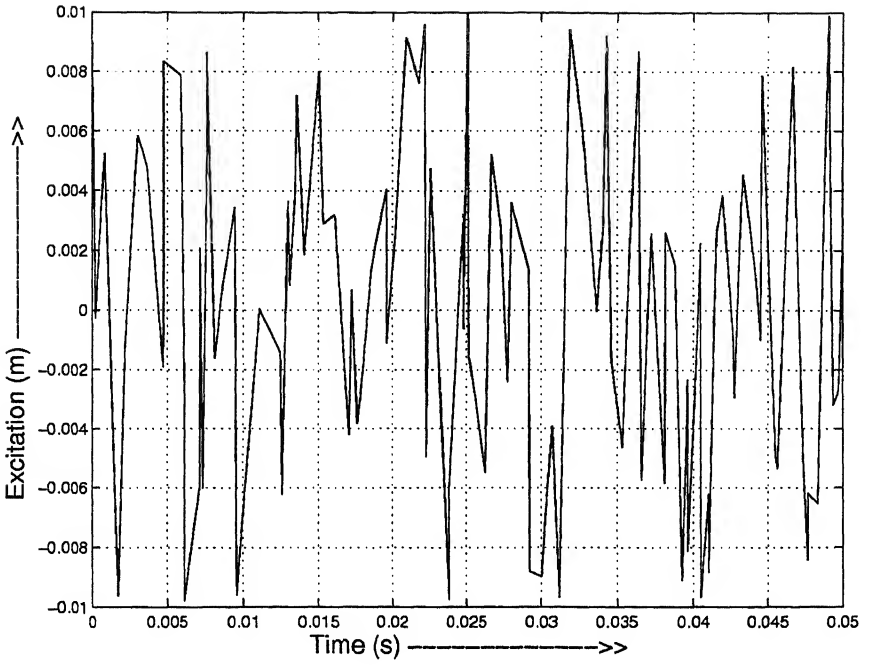

Figure 5.9: Base Excitation

system. This control strategy can be used for vibration isolation in many applications e.g. isolating telescopes from surrounding disturbances, maintaining the desired direction of the naval missiles, etc. After the simulations give satisfactory results, then, the controller should be fabricated to control the disturbances. Since the flexibilities of legs are considered here, the numerical simulations are closer to the physical system.

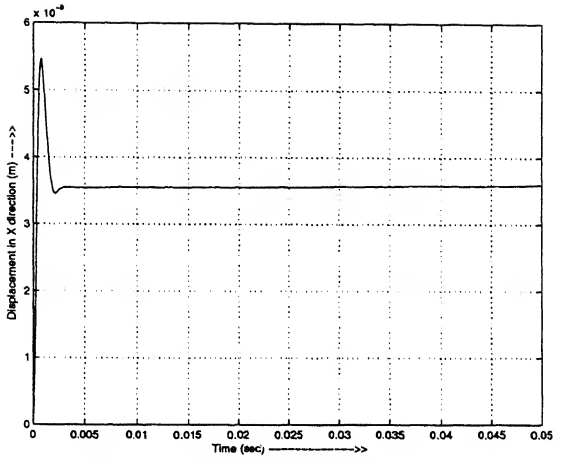

Translation in X direction

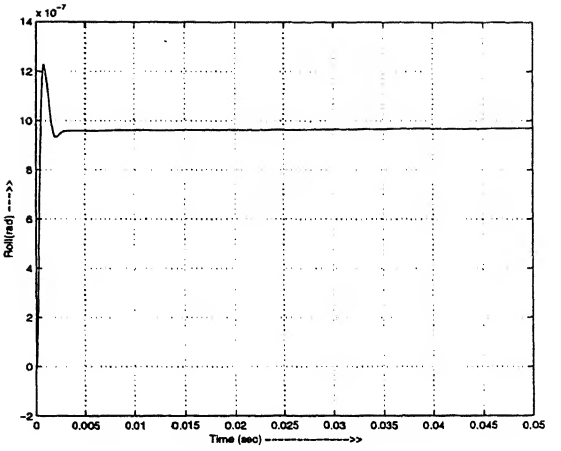

Rotation about X axis

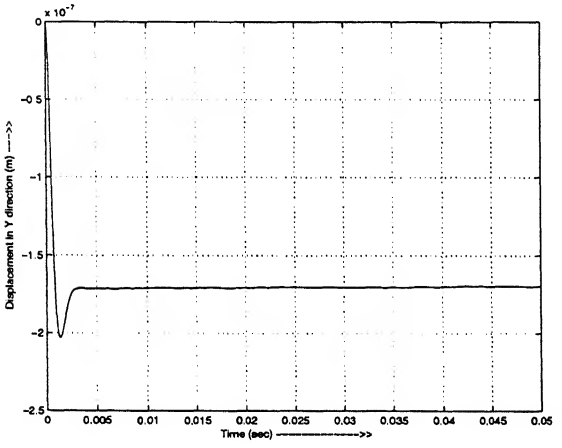

Translation in Y direction

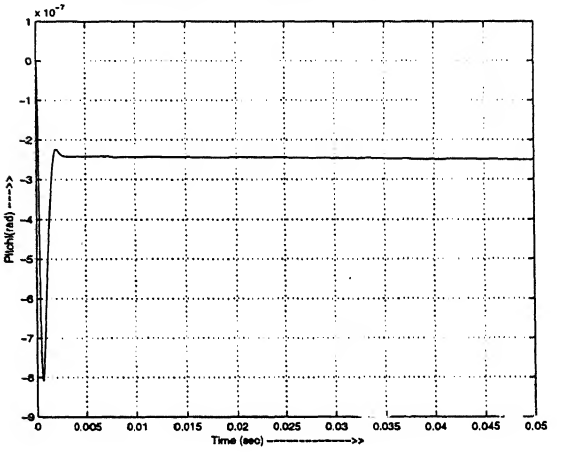

Rotation about Y axis

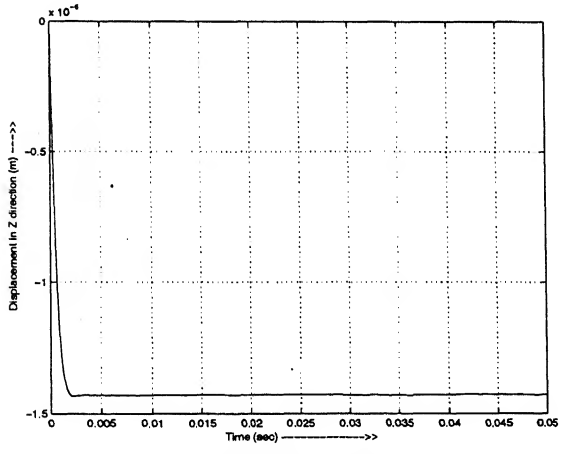

Translation in Z direction

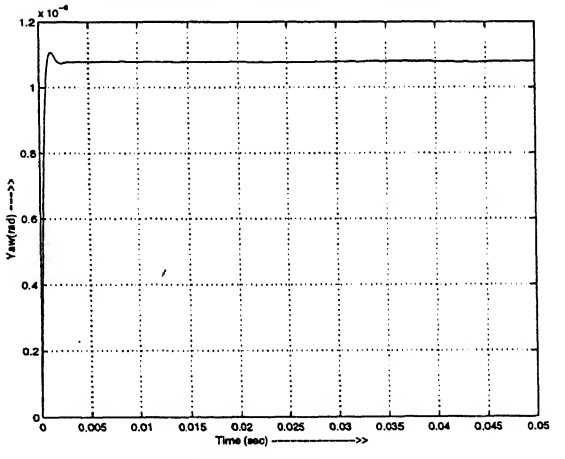

Rotation about Z axis

Figure 5.10: Control of Vibration Due to Random Base Excitation (Test Manipulator II)

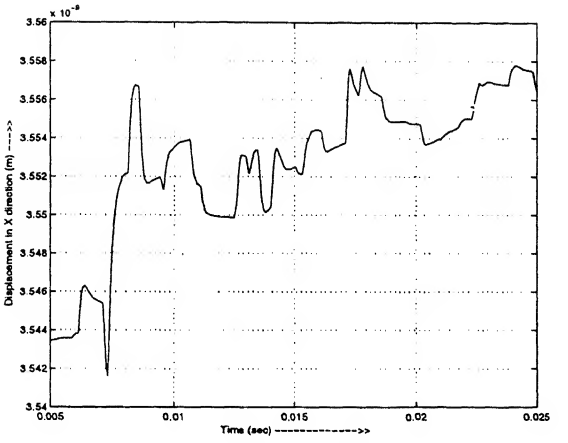

Translation in X direction

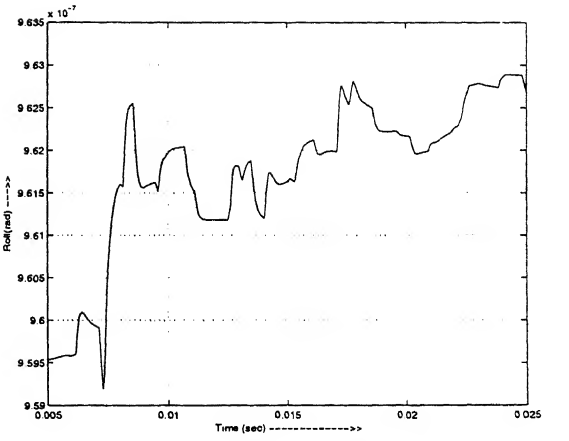

Rotation about X axis

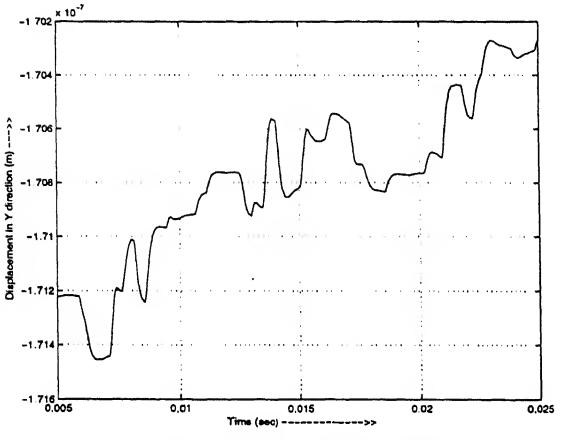

Translation in Y direction

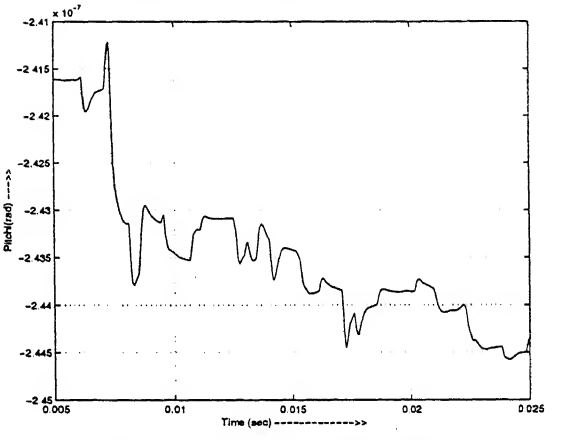

Rotation about Y axis

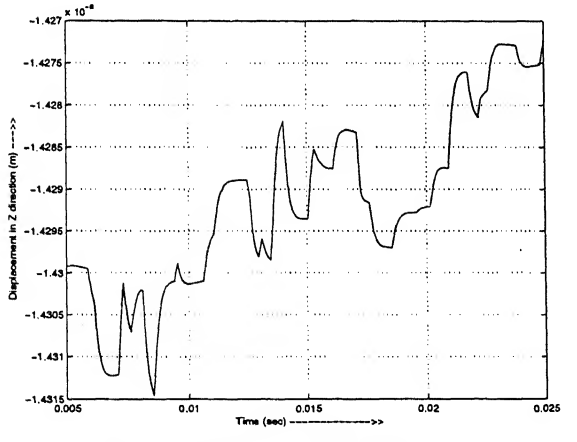

Translation in Z direction

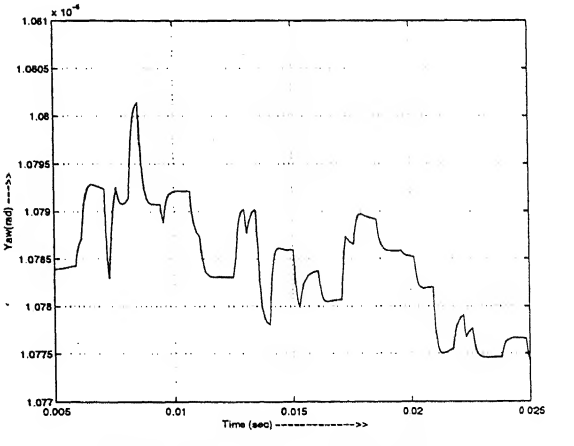

Rotation about Z axis

Figure 5.11: Zoomed from Fig. (5.10), between 0.005 sec. to 0.025 sec (Test Manipulator II)

Chapter 6

Closure

6.1 Summary

In this thesis, singularity measures of a manipulator, dynamics and vibrations of the Stewart platform have been investigated. Finally, a vibration control strategy has been developed using 6-UPS Stewart platforms. Numerical simulations have been performed to evaluate the controller's performance.

In chapter 1, a comparison between parallel and serial manipulators and a brief description of Stewart platform have been presented. Then the state of the arts have been discussed.

In chapter 2, a dynamic stability index is introduced and compared with conventional measure of static singularity. Though this is illustrated with 6-UPS Stewart platform, it can also be used for other parallel manipulators.

In chapter 3, considering the motion of the base platform and flexibility of the legs, a generalized closed form dynamic equation of 6-UPS Stewart platform has been developed following the Newton-Euler approach. Using this equations a vibration study of Stewart platform has been performed in chapter 4.

In chapter 5, an active vibration control strategy using Stewart platform has been presented. A linearized model has also been developed to calculate the gains of PD controller. Finally, simulations of vibration isolation have been done using data of some standard Stewart platforms.

6.2 Suggestions for Future Work

The work of this thesis can be extended in many directions. A few among them which may have quite significant outcomes, are discussed below.

1. In chapter 2 significances of the lowest natural frequency of manipulators have been discussed. This can be used at the time of designing a manipulator so that manipulators, used for a particular pose have a high value of the lowest natural frequency at the desired configuration and manipulators designed for tracking purpose should have a high value of the lowest natural frequency over the whole path in an overall sense.

2. The dynamic equation (Eqn. 3.48), derived in the chapter 3, can be non-dimensionalized. It will reduce some parameters and also the behaviour of the platform can be predicted in terms of non-dimensional parameters. Hence, comparison between two different designs of Stewart platform will be much more convenient and accurate. Moreover, one analysis will apply to a class of Stewart platform. Scale up or scale down version of a model will not need separate analysis.

3. The generality of the formulation of chapter 3 can be further extended by incorporating distribution of the stiffness over the whole leg. Use of *Finite Element* and *Finite Difference* method will be quite useful in this case. The computation overhead of the FE and FD models can be handled by using parallel programming

4. In chapter 4, vibration study has been done up to little above the 2nd natural frequency. As the simulations have been done in MATLAB, requirements of computation time is quite high. Using lower level programming languages (C, C++, FORTRAN, etc.) with parallel programming, this impediment can be removed and the work can be extended to find out response of the top platform at the base excitation frequency above the second natural frequency. Thus, Fig. (4.3) can be completed. The behaviour of the top platform at the natural frequencies also can be studied in more details.

5. In chapter 5, vibration isolation has been done using PD controller. For trajectory tracking purpose feedforward strategy can be used. Besides, other control strategies i.e. PID, Neural Network, Fuzzy logic etc., can be explored in the future work in this field.

Bibliography

[1] S. Bhattacharya, H. Hatwal, and A. Ghosh. Comparison of an exact and an approximate method of singularity avoidance in platform type parallel manipulator. *Mechanism and Mechine Theory*, 33(7):965 – 974, Oct. 1998.

[2] Y. Cheng, G. Ren, and S. Dai. The multi-body system modelling of the Gough-Stewart platform for vibration control. *Journal of Sound and Vibration*, 271(3 - 5):599 – 614, Apr. 2004.

[3] John J. Craig. *Introduction to Robotics Mlechanics and Control.* Pearson Education, second edition edition, 2003.

[4] B. Dasgupta and T. S. Mruthyunjaya. A Newton-Euler formulation for the inverse dynamics of the Stewart platform manipulator. *Mechanism and Mechine Theory*, 33(8):1135 – 1152, Nov. 1998.

[5] B. Dasgupta and T. S. Mruthyunjaya. Closed-form dynamic equation of the general Stewart platform through the Newton-Euler approach. *Mechanism and Mechine Theory*, 33(7):993 – 1012, Oct. 1998.

[6] B. Dasgupta and T. S. Mruthyunjaya. Force redundancy in parallel manipulators: theoretical and practical issues. *Mechanism and Mechine Theory*, 33(6):727 – 742, Aug. 1998.

[7] B. Dasgupta and T. S. Mruthyunjaya. Singularity-free path planning for the Stewart platform manipulator. *Mechanism and Mechine Theory*, 33(6):711 – 725, Aug. 1998.

[8] T. A. Dwarkanath, Bhaskar Dasgupta, and T. S. Mruthyunjaya. Design and development of a Stewart platform based force-torque sensor. *Mechatronics*, 11.

[9] E. F. Fichter. The Stewart platform manipulator: general theory and practical construction. *International Journal of Robotics Research*, 5(2):157 – 182, 1986.

[10] K. S. Fu, R. C. Gonzalez, and C. S. G. Lee. *ROBOTICS Control, Sensing, Vision and Intelligence*. McGraw-Hill Book Company, first edition edition, 1988.

[11] Z. Geng, L. S. Haynes, D. Lee, and R. L. Carroll. On the dynamic model and kinematic analysis of a class of Stewart platforms. *Robotics and Autonomous Systems*, 9(4):237 – 254, 1992.

[12] Z. J. Geng and L. S. Haynes. Six degree-of-freedom active vibration control using the Stewart platform. *IEEE trans. on control systems technology*, 2(1):45 – 53, Mar. 1994.

[13] R. Gexue, L. Qiuhai, H. Ning, N. Rendong, and P. Bo. On vibration control with Stewart parallel mechanism. *Mechatronics*, 14(1):1 – 13, Feb. 2004.

[14] C. Gosselin. Stiffness mapping of parallel manipulators. *IEEE trans. Robot. Automn.*, 6(3):377 – 382, Jun. 1990.

[15] C. Gosselin and J. Angeles. Singularity analysis of closed-loop kinematic chains. *IEEE Trans. Robot. Automn*, 6(3):281 – 290, Jun. 1990.

[16] V. E. Gough and S. G. Whitehall. Universal tyre testing machine. *Proc. of 9-th International Tech. Congress F.I.S.I.T.A.*, 117, 1962.

[17] N. I. Kim and C. W. Lee. Multi axis vibration control of a slender structure by using the Stewart platform manipulator. *Mechanism and Mechine Theory*, 36(11 - 12):1253 – 1269, Nov. 2001.

[18] E. Kreyszig. *Advanced Engineering Mathematics*. John wiley and Sons.

[19] G. Lebret, K. Liu, and F. L. Lewis. Dynamic analysis and control of a Stewart platform manipulator. *Journal of Robotic Systems*, 10(5):629 – 655, Jul. 1993.

[20] J. D. Lee and J. Z. Geng. A dynamic model of a flexible Stewart platform. *Computers and Structures*, 48(3):367 – 374, Aug. 1993.

[21] S. H. Lee, J. B. Song, W. C. Choi, and D. Hong. Position control of a Stewart platform using inverse dynamics control with approximate dynamics. *Mechatronics*, 13(6):605 – .619, Jul. 2003.

[22] O. Ma and J. Angeles. The concept of dynamic isotropy and its applications to inverse kinematics and trajectory planning. *in: Proc. IEEE Int. Conf. Robot. Autumn.*, 1:470 – 475, May 1990.

[23] O. Ma and J. Angeles. Architecture singularities of platform manipulators. *in: Proc. IEEE Int. Conf. Robot. Autumn.*, pages 1542 – 1547, Apr. 1991.

[24] O. Ma and J. Angeles. Optimum design of manipulator under dynamic isotropy condition. *in: Proc. IEEE Int. Conf. Robot. Autumn.*, 1:470 - 475, May 1993.

[25] H. McCallion and P. D. Truong. The analysis of a six-degrees-of-freedom workstation for mechanized assembly. *Proc. of 5-th World Congress on the Theory of Mechines and Mechanisms (IFToMM)*, pages 611 – 616, 1979.

[26] J. E. McInroy. Modeling and design of flexure jointed Stewart platforms for control purpose. *IEEE/ASME Trans, on Mechatronics*, 7(1):95 - 99, Mar. 2002.

[27] L. Meirovitch. *Elements of Vibration Analysis.* McGraw-Hill.

[28] L. Meirovitch. *Analytical Methods in Vibrations.* Prentice Hall, first edition edition, 1997.

[29] J. P. Merlet. Parallel manipulators, Part 1: Theory, design, kinematics, dynamics and control. *INRIA Research Report, No. 646*, 1987.

[30] Katsukhio Ogata. *Modern Control Engineering.* Prentice Hall, third edition edition, 2000.

[31] W. H. Press, S. A. Teukolsky, W. T. Vetterling, and B. P. Flannery. *Numerical Recipes in C++ The Art of Scientific Computing.* Cambridge University Press, second edition edition, 2003.

[32] J. M. Selig and X. Ding. Theory of vibration in Stewart platform. In *Proc. of the IEEE International Conference on Intelligent Robots and Systems*, pages 2190 –2195, Maui, Hawali, USA, Oct.29 - Nov.03 2001.

[33] Shuguang and J. M. Schimmels. The bounds and realization of spatial stiffness achieved with simple springs connected in parallel. *IEEE trans. on Robot.and Automn.*, 14(3), Jun. 1998.

[34] G. F. Simmons. *Differential Equations with Applications and Historical Notes.* McGraw-Hill Education, second edition edition, 2003.

[35] D. Stewart. A platform with six degrees of freedom. *Proc. of Instite of Mechanical Engineers*, 180(17):371 – 386, 1965.

[36] W. T. Thomson. *Theory of Vibration with Applications.* Prentice Hall.

[37] D. C. H. Yang and T. W. Lee. Feasibility study of a platform type of robotic manipulators from kinematic standpoint. *ASME Trans, J. Mech. Transm. Automn Des*, 106:191 – 198, 1984,.

[38] Y.Nakamura. *Advanced Robotics: Redundancy and Optimization.* Addison-Wesley, 1991.

[39] T. Yoshikawa. Dynamic manipulability of robot manipulators. *IEEE Conf. Decision and Control*, 2:1033 – 1038, Mar. 1985.

[40] C. D. Zhang and S. M. Song. An efficient method for inverse dynamics of manipulators based on the virtual work principle. *Journal of Robotic Systems*, 10(5):605 – 627, Jul. 1993.

Appendix A

Description of the Test Manipulators

A.1 Test Manipulator I

All data are in SI unit.

Base points:

$$[\ \mathbf{b}_1\ \ \mathbf{b}_2\ \ \mathbf{b}_3\ \ \mathbf{b}_4\ \ \mathbf{b}_5\ \ \mathbf{b}_6\ ] = \begin{bmatrix} 0.6 & 0.1 & -0.3 & -0.3 & 0.20 & 0.5 \\ 0.2 & 0.5 & 0.3 & -0.4 & -0.30 & -0.2 \\ 0.0 & 0.1 & 0.1 & 0.0 & -0.05 & 0.0 \end{bmatrix}$$

Platform points (in platform frame):

$$[\ \mathbf{p}_1\ \ \mathbf{p}_2\ \ \mathbf{p}_3\ \ \mathbf{p}_4\ \ \mathbf{p}_5\ \ \mathbf{p}_6\ ] = \begin{bmatrix} 0.3 & 0.3 & 0.0 & -0.2 & -0.15 & 0.15 \\ 0.0 & 0.2 & 0.3 & 0.1 & -0.20 & -0.15 \\ 0.1 & 0.0 & 0.0 & -0.1 & -0.05 & -0.05 \end{bmatrix}$$

Unit vectors along fixed axes of universal joints:

$$[\ \overline{\mathbf{k}}_1\ \ \overline{\mathbf{k}}_2\ \ \overline{\mathbf{k}}_3\ \ \overline{\mathbf{k}}_4\ \ \overline{\mathbf{k}}_5\ \ \overline{\mathbf{k}}_6\ ] = \begin{bmatrix} -0.8141 & 0.2308 & 0.9535 & 1.0000 & 0.7071 & -0.9535 \\ 0.2714 & 0.9231 & 0.2860 & 0.0000 & 0.7071 & 0.2860 \\ 0.0000 & 0.3077 & 0.0953 & 0.0000 & 0.0000 & -0.0953 \end{bmatrix}$$

Mass of lower and upper part of each leg:

$$m_d = 3.0 \quad \text{and} \quad m_u = 1.0$$

Centers of gravity of lower and upper parts of each leg (in local frames):

$$\mathbf{r}_{d_0} = [\ 0.4\ \ 0.14\ \ -0.18\ ]^T \quad \text{and} \quad \mathbf{r}_{u_0} = [\ -6.0\ \ -0.08\ \ 0.08\ ]^T$$

Moments of inertia of lower and upper parts of each leg (in local frames):

$$\mathbf{I}_{d_0} = \begin{bmatrix} 0.010 & 0.005 & 0.007 \\ 0.005 & 0.002 & 0.003 \\ 0.007 & 0.003 & 0.001 \end{bmatrix} \quad \text{and} \quad \mathbf{I}_{u_0} = \begin{bmatrix} 0.005 & 0.002 & 0.002 \\ 0.002 & 0.002 & 0.001 \\ 0.002 & 0.001 & 0.003 \end{bmatrix}$$

Centre of gravity of the platform and payload (in platform frame):

$$\mathbf{R}_0 = \begin{bmatrix} 0.04 & 0.03 & -0.06 \end{bmatrix}^T$$

Moment of inertia of platform and payload (in platform frame):

$$\mathbf{I}_p = \begin{bmatrix} 0.050 & 0.003 & 0.004 \\ 0.003 & 0.040 & 0.003 \\ 0.004 & 0.003 & 0.100 \end{bmatrix}$$

Coefficients of viscous friction:

$$C_u = 0.0001, \qquad C_p = 0.001, \qquad C_s = 0.0002$$

Stiffness of legs:

$$\begin{aligned} K_{leg_1} &= 2 \times 10^8 \\ K_{leg_2} &= 2 \times 10^8 \\ K_{leg_3} &= 2 \times 10^8 \\ K_{leg_4} &= 2 \times 10^8 \\ K_{leg_5} &= 2 \times 10^8 \\ K_{leg_6} &= 2 \times 10^8 \end{aligned}$$

A.2 Test Manipulator II

All data are in SI unit.

Base points:

$$\begin{bmatrix} \mathbf{b}_1 & \mathbf{b}_2 & \mathbf{b}_3 & \mathbf{b}_4 & \mathbf{b}_5 & \mathbf{b}_6 \end{bmatrix} = \begin{bmatrix} 0.03 & 0.004486 & -0.015 & -0.02793 & -0.015 & 0.02345 \\ 0.00 & 0.02966 & 0.02598 & -0.01095 & -0.02598 & -0.01872 \\ 0.00 & 0.0 & 0.0 & 0.00 & -0.0 & 0.0 \end{bmatrix}$$

Platform points (in platform frame):

$$\begin{bmatrix} \mathbf{p}_1 & \mathbf{p}_2 & \mathbf{p}_3 & \mathbf{p}_4 & \mathbf{p}_5 & \mathbf{p}_6 \end{bmatrix} = \begin{bmatrix} 0.0428 & 0.0326 & -0.0334 & -0.0432 & -0.0094 & 0.0106 \\ 0.0139 & 0.0313 & 0.0301 & 0.0127 & -0.0440 & -0.0437 \\ 0.0 & 0.0 & 0.0 & 0.0 & 0.0 & 0.0 \end{bmatrix}$$

Mass of lower and upper part of each leg:

$$m_d = 0.3 \quad \text{and} \quad m_u = 0.1$$

Centers of gravity of lower and upper parts of each leg (in local frames):

$$\mathbf{r}_{d_0} = \begin{bmatrix} 0.04 & 0.014 & -0.018 \end{bmatrix}^T \quad \text{and} \quad \mathbf{r}_{u_0} = \begin{bmatrix} -0.6 & -0.008 & 0.008 \end{bmatrix}^T$$

Moments of inertia of lower and upper parts of each leg (in local frames):

$$\mathbf{I}_{d_0} = \begin{bmatrix} 0.000010 & 0.000005 & 0.000007 \\ 0.000005 & 0.000002 & 0.000003 \\ 0.000007 & 0.000003 & 0.000001 \end{bmatrix} \quad \text{and} \quad \mathbf{I}_{u_0} = \begin{bmatrix} 0.000005 & 0.000002 & 0.000002 \\ 0.000002 & 0.000002 & 0.000001 \\ 0.000002 & 0.001 & 0.003 \end{bmatrix}$$

Centre of gravity of the platform and payload (in platform frame):

$$\mathbf{R}_0 = \begin{bmatrix} 0 & 0 & 0 \end{bmatrix}^T$$

Moment of inertia of platform and payload (in platform frame):

$$\mathbf{I}_p = \begin{bmatrix} 0.0001 & 0.0 & 0.0 \\ 0.0 & 0.0001 & 0.0 \\ 0.0 & 0.0 & 0.0001 \end{bmatrix}$$

Coefficients of viscous friction:

$$C_u = 0.0001, \qquad C_p = 0.001, \qquad C_s = 0.0002$$

Stiffness of legs:

$$\begin{aligned} K_{leg_1} &= 8 \times 10^7 \\ K_{leg_2} &= 8 \times 10^7 \\ K_{leg_3} &= 8 \times 10^7 \\ K_{leg_4} &= 8 \times 10^7 \\ K_{leg_5} &= 8 \times 10^7 \\ K_{leg_6} &= 8 \times 10^7 \end{aligned}$$

All other parameters are same as of previous section.

Appendix B

Jacobian Expression

Jacobian expression ($\mathbf{A}$), required for devloping the linearized model of the chapter 5, is developed here.

$$\mathbf{A}(1:6,1:6) = \mathbf{0} \tag{B.1}$$

$$\mathbf{A}(1:6,7:12) = [6 \times 6] \text{ Identity Matrix} \tag{B.2}$$

Let,

$$\mathbf{a} = \mathbf{J}_p^{-1}\left(\mathbf{HF} + \begin{bmatrix} \Re_p \mathbf{F}_{ext} \\ \Re_p \mathbf{M}_{ext} \end{bmatrix} - \eta + \mathbf{d}\right) \tag{B.3}$$

and,

$$\mathbf{A}(7:12,1:12) = \mathbf{D} \tag{B.4}$$

Hence, i-th column of $\mathbf{D}$ is

$$\mathbf{D}_i = \mathbf{J}_p^{-1}\frac{\partial \mathbf{a}}{\partial z_i} + \frac{\partial \mathbf{J}_p^{-1}}{\partial z_i}\mathbf{a} \tag{B.5}$$

Partial differentiation of inverse of a complicated matrix like $\mathbf{J}$ is very difficult. But it can be simplified by using the following algebraic rule.

$$\frac{\partial \mathbf{J}_p^{-1}}{\partial z_i} = -\mathbf{J}_p^{-1}\frac{\partial \mathbf{J}_p}{\partial z_i}\mathbf{J}_p^{-1}. \tag{B.6}$$

So Eqn. (B.5) becomes,

$$\begin{aligned} \mathbf{D}_i &= \mathbf{J}_p^{-1}\frac{\partial \mathbf{a}}{\partial z_i} - \mathbf{J}_p^{-1}\frac{\partial \mathbf{J}_p}{\partial z_i}\mathbf{J}_p^{-1}\mathbf{a} \\ &= \mathbf{J}_p^{-1}\left(\frac{\partial \mathbf{a}}{\partial z_i} - \frac{\partial \mathbf{J}_p}{\partial z_i}\mathbf{J}_p^{-1}\mathbf{a}\right) \end{aligned} \tag{B.7}$$

where

$$\frac{\partial \mathbf{a}}{\partial z_i} = \frac{\partial(\mathbf{HF})}{\partial z_i} - \frac{\partial \eta}{\partial z_i} + \frac{\partial}{\partial z_i}\begin{bmatrix} \Re_p \mathbf{F}_{ext} \\ \Re_p \mathbf{M}_{ext} \end{bmatrix} \tag{B.8}$$

$$\frac{\partial \mathbf{J}_{p_i}}{\partial z_i} = \frac{\partial \mathbf{J_{plat}}}{\partial z_i} + \frac{\partial}{\partial z_i}\sum_{j=1}^{6} \mathbf{J}_{p_j} \tag{B.9}$$

$\mathbf{J_{plat}}$ = Moment of inertia of top platform.

$\mathbf{J}_{p_j}$ = Moment of inertia of j-th leg.

$$\frac{\partial \mathbf{J_{plat}}}{\partial z_i} = \begin{bmatrix} \frac{\partial M \mathbf{E}_3}{\partial z_i} & -\frac{\partial M \widetilde{\mathbf{R}}_p}{\partial z_i} \\ \frac{\partial M \widetilde{\mathbf{R}}_p}{\partial z_i} & \frac{\partial}{\partial z_i}\{\mathbf{I} + M(R_p^2 \mathbf{E}_3 - \mathbf{R}_p \mathbf{R}_p^T)\} \end{bmatrix} \tag{B.10}$$

$$\frac{\partial M \mathbf{E}_3}{\partial z_i} = \mathbf{0} \tag{B.11}$$

$$\frac{\partial M \widetilde{\mathbf{R}}}{\partial z_i} = M \frac{\partial}{\partial z_i} \widetilde{\Re_p \mathbf{R}_0} \tag{B.12}$$

$\frac{\partial \Re_p}{\partial z_i} = \mathbf{0}$ for $i \neq 4,\ 5$ or 6

$$\frac{\partial \Re_p}{\partial z_4} = \begin{bmatrix} 0 & c(z_6)s(z_5)c(z_4) + s(z_6)s(z_4) & -c(z_6)s(z_5)s(z_4) + s(z_6)c(z_4) \\ 0 & s(z_6)s(z_5)c(z_4) - c(z_6)s(z_4) & -s(z_6)s(z_5)s(z_4) - c(z_6)c(z_4) \\ 0 & c(z_5)c(z_4) & -c(z_5)s(z_4) \end{bmatrix}$$

$$\frac{\partial \Re_p}{\partial z_5} = \begin{bmatrix} -c(z_6)s(z_5) & c(z_6)c(z_5)s(z_4) & c(z_6)c(z_5)c(z_4) \\ -s(z_6)s(z_5) & s(z_6)c(z_5)s(z_4) & s(z_6)c(z_5)c(z_4) \\ -c(z_5) & -s(z_5)s(z_4) & -s(z_5)c(z_4) \end{bmatrix}$$

$$\frac{\partial \Re_p}{\partial z_6} = \begin{bmatrix} -s(z_6)c(z_5) & -s(z_6)s(z_5)s(z_4) - c(z_6)c(z_4) & -s(z_6)s(z_5)c(z_4) + c(z_6)s(z_4) \\ c(z_6)c(z_5) & c(z_6)s(z_5)s(z_4) - s(z_6)c(z_4) & c(z_6)s(z_5)c(z_4) + s(z_6)s(z_4) \\ 0 & 0 & 0 \end{bmatrix}$$

Where, $c(.) \equiv \cos(.)$ and $s(.) \equiv \sin(.)$.

The (2,2) element of $\mathbf{J_{plat}}$ [in Eqn. (B.10)] is

$$\begin{aligned} \frac{\partial}{\partial z_i}\{\mathbf{I} + M(R_p^2 \mathbf{E}_3 - \mathbf{R}_p \mathbf{R}_p^T)\} &= \frac{\partial \Re_p}{\partial z_i} \mathbf{I}_p \Re_p^T + \Re_p \mathbf{I}_p (\frac{\partial \Re_p}{\partial z_i})^T \\ &\quad + M\{\mathbf{R}_{0_p}^T (\frac{\partial \Re_p}{\partial z_i})^T \mathbf{R}_p \mathbf{E}_3 + \mathbf{R}_p^T \frac{\partial \Re_p}{\partial z_i} \mathbf{R}_{0_p} \mathbf{E}_3 - \frac{\partial \Re_p}{\partial z_i} \mathbf{R}_{0_p} \mathbf{R}_p^T \\ &\quad - \mathbf{R}_p \mathbf{R}_{0_p}^T (\frac{\partial \Re_p}{\partial z_i})^T\}. \end{aligned} \tag{B.13}$$

Using expressions (B.11), (B.12) and (B.13) we can find out the expression of $\frac{\partial \mathbf{J_{plat}}}{\partial z_i}$ from Eqn. (B.10).

Expanding the 2nd term of expression (B.9) we get,

$$\frac{\partial \mathbf{J}_{p_j}}{\partial z_i} = \begin{bmatrix} \frac{\partial \mathbf{Q}_{p_j}}{\partial z_i} & -\frac{\partial(\mathbf{Q}_{p_j}\tilde{\mathbf{q}}_{p_j})}{\partial z_i} \\ \frac{\partial(\tilde{\mathbf{q}}_{p_j}\mathbf{Q}_{p_j})}{\partial z_i} & -\frac{\partial(\tilde{\mathbf{q}}_{p_j}\mathbf{Q}_{p_j}\tilde{\mathbf{q}}_{p_j})}{\partial z_i} \end{bmatrix}$$

$$= \begin{bmatrix} \frac{\partial \mathbf{Q}_{p_j}}{\partial z_i} & -(\frac{\partial \mathbf{Q}_{p_j}}{\partial z_i}\tilde{\mathbf{q}}_{p_j} + \mathbf{Q}_{p_j}\frac{\partial \tilde{\mathbf{q}}_{p_j}}{\partial z_i}) \\ \frac{\partial \tilde{\mathbf{q}}_{p_j}}{\partial z_i}\mathbf{Q}_{p_j} + \tilde{\mathbf{q}}_{p_j}\frac{\partial \mathbf{Q}_{p_j}}{\partial z_i} & -(\frac{\partial \tilde{\mathbf{q}}_{p_j}}{\partial z_i}\mathbf{Q}_{p_j}\tilde{\mathbf{q}}_{p_j} + \tilde{\mathbf{q}}_{p_j}\frac{\partial \mathbf{Q}_{p_j}}{\partial z_i}\tilde{\mathbf{q}}_{p_j} + \tilde{\mathbf{q}}_{p_j}\mathbf{Q}_{p_j}\frac{\partial \tilde{\mathbf{q}}_{p_j}}{\partial z_i}) \end{bmatrix} \quad \text{(B.14)}$$

Other than $\frac{\partial \mathbf{q}_{p_j}}{\partial z_i}$ and $\frac{\partial \mathbf{Q}_{p_j}}{\partial z_i}$ all terms of the Eqn. (B.14) are known.

$$\frac{\partial \mathbf{q}_{p_j}}{\partial z_i} = \frac{\partial \Re_p}{\partial z_i}\mathbf{p}_j \quad \text{(B.15)}$$

At the time of developing expressions for $\frac{\partial \mathbf{Q}_j}{\partial z_i}$, the suffixes ($i$ and j) have been dropped to reduce the cluttering of the expressions. Before going into derivation of $\frac{\partial \mathbf{Q}_j}{\partial z_i}$, those expressions which are required for derivation have been evaluated below.

$$\frac{\partial L}{\partial z} = \frac{1}{2L}[\{(\frac{\partial \mathbf{q}_p}{\partial z} + \frac{\partial \mathbf{t}_p}{\partial z}) - (\frac{\partial \mathbf{q}_b}{\partial z} + \frac{\partial \mathbf{t}_b}{\partial z})\}^T\mathbf{S} + \mathbf{S}^T(\frac{\partial \mathbf{q}_p}{\partial z} + \frac{\partial \mathbf{t}_p}{\partial z})] \quad \text{(B.16)}$$

$$\frac{\partial \mathbf{s}}{\partial z} = \frac{1}{L^2}\{(\frac{\partial \mathbf{q}_p}{\partial z} + \frac{\partial \mathbf{t}_p}{\partial z})L - \frac{\partial L}{\partial z}\mathbf{S}\} \quad \text{(B.17)}$$

$$\frac{\partial \parallel \mathbf{k}\times\mathbf{s} \parallel}{\partial z} = \frac{1}{2 \parallel \mathbf{k}\times\mathbf{s} \parallel}\{(\mathbf{k}\times\frac{\partial \mathbf{s}}{\partial z})^T(\mathbf{k}\times\mathbf{s}) + (\mathbf{k}\times\mathbf{s})^T(\mathbf{k}\times\frac{\partial \mathbf{s}}{\partial z})\} \quad \text{(B.18)}$$

$$\frac{\partial \mathbf{T}}{\partial z} = \frac{\partial}{\partial z}\begin{bmatrix} \mathbf{s} & \frac{\mathbf{k}\times\mathbf{s}}{\parallel \mathbf{k}\times\mathbf{s} \parallel} & \frac{\mathbf{s}\times(\mathbf{k}\times\mathbf{s})}{\parallel \mathbf{k}\times\mathbf{s} \parallel} \end{bmatrix} \quad \text{(B.19)}$$

$$\frac{\partial}{\partial z}\{\tilde{\mathbf{s}}(\mathbf{I}_d + \mathbf{I}_u)\tilde{\mathbf{s}}\} = \frac{\partial \tilde{\mathbf{s}}}{\partial z}(\mathbf{I}_d + \mathbf{I}_u)\tilde{\mathbf{s}} + \tilde{\mathbf{s}}(\frac{\partial \mathbf{I}_d}{\partial z} + \frac{\partial \mathbf{I}_u}{\partial z})\tilde{\mathbf{s}} + \tilde{\mathbf{s}}(\mathbf{I}_d + \mathbf{I}_u)\frac{\partial \tilde{\mathbf{s}}}{\partial z} \quad \text{(B.20)}$$

We can break $\frac{\partial \mathbf{Q}_p}{\partial z}$ in the four following terms.

$$\frac{\partial \mathbf{Q}_p}{\partial z} = \text{Term1} + \text{Term2} - \text{Term3} - \text{Term4} \quad \text{(B.21)}$$

Where

$$\text{Term1} = [2m_u\frac{(\frac{\partial \mathbf{s}}{\partial z}.\mathbf{r}_u + \mathbf{s}.\frac{\partial \mathbf{s}}{\partial z})L - \frac{\partial L}{\partial z}(\mathbf{s}.\mathbf{r}_u)}{L^2}$$
$$-\frac{\{m_d((\frac{\partial \mathbf{r}_d}{\partial z})^T\mathbf{r}_d + \mathbf{r}_d^T\frac{\partial \mathbf{r}_d}{\partial z}) + m_u((\frac{\partial \mathbf{r}_u}{\partial z})^T\mathbf{r}_u + \mathbf{r}_u^T\frac{\partial \mathbf{r}_u}{\partial z})\}L^2 - 2L\frac{\partial L}{\partial z}(m_d r_d^2 + m_u r_u^2)}{L^4}]\mathbf{s}\mathbf{s}^T$$
$$+[m_u(1 + \frac{2\mathbf{s}.\mathbf{r}_u}{L}) - \frac{(m_d r_d^2 + m_u r_u^2)}{L^2}]\{\frac{\partial \mathbf{s}}{\partial z}\mathbf{s}^T + \mathbf{s}(\frac{\partial \mathbf{s}}{\partial z})^T\} \quad \text{(B.22)}$$

$$\text{Term2} = \frac{1}{L^4}\mathbf{E}_3[\{m_d((\frac{\partial \mathbf{r}_d}{\partial z})^T\mathbf{r}_d + \mathbf{r}_d^T\frac{\partial \mathbf{r}_d}{\partial z}) + m_u((\frac{\partial \mathbf{r}_u}{\partial z})^T\mathbf{r}_u + \mathbf{r}_u^T\frac{\partial \mathbf{r}_u}{\partial z})\}L^2$$

$$-2L\frac{\partial L}{\partial z}(m_d r_d^2 + m_u r_u^2)] \tag{B.23}$$

$$\text{Term3} = \frac{m_u}{L^2}[\{\frac{\partial \mathbf{s}}{\partial z}\mathbf{r}_u^T + \mathbf{s}(\frac{\partial \mathbf{r}_u}{\partial z})^T + \frac{\partial \mathbf{r}_u}{\partial z}\mathbf{s}^T + \mathbf{r}_u(\frac{\partial \mathbf{s}}{\partial z})^T\}L - \frac{\partial L}{\partial z}(\mathbf{s}\mathbf{r}_u^T + \mathbf{r}_u\mathbf{s}^T)] \tag{B.24}$$

$$\begin{aligned}\text{Term4} = \frac{1}{L^4}[L^2\{m_d[(\frac{\partial \mathbf{s}}{\partial z}\times\mathbf{r}_d + \mathbf{s}\times\frac{\partial \mathbf{r}_d}{\partial z})(\mathbf{s}\times\mathbf{r}_d)^T + (\mathbf{s}\times\mathbf{r}_d)(\frac{\partial \mathbf{s}}{\partial z}\times\mathbf{r}_d + \mathbf{s}\times\frac{\partial \mathbf{r}_d}{\partial z})^T] \\ + m_u[(\frac{\partial \mathbf{s}}{\partial z}\times\mathbf{r}_u + \mathbf{s}\times\frac{\partial \mathbf{r}_u}{\partial z})(\mathbf{s}\times\mathbf{r}_u)^T + (\mathbf{s}\times\mathbf{r}_u)(\frac{\partial \mathbf{s}}{\partial z}\times\mathbf{r}_u + \mathbf{s}\times\frac{\partial \mathbf{r}_u}{\partial z})^T] \\ + \frac{\partial}{\partial z}[\tilde{\mathbf{s}}(\mathbf{I}_d + \mathbf{I}_u)\tilde{\mathbf{s}}]\} - \{m_d(\mathbf{s}\times\mathbf{r}_d)(\mathbf{s}\times\mathbf{r}_d)^T + m_u(\mathbf{s}\times\mathbf{r}_u)(\mathbf{s}\times\mathbf{r}_u)^T \\ + \tilde{\mathbf{s}}(\mathbf{I}_d + \mathbf{I}_u)\tilde{\mathbf{s}}\}2L\frac{\partial L}{\partial z}]\end{aligned} \tag{B.25}$$

Using Eqn. (B.16), (B.17), (B.19), (B.20) and Eqn. (B.22) to (B.25) we can express $\frac{\partial \mathbf{Q}_{p_j}}{\partial z_i}$ in terms of platform parameters and $\mathbf{z}$. Again using Eqn. (B.15) we can evaluate $\frac{\partial \mathbf{J}_{p_j}}{\partial z_i}$. Hence, this completes the expression of $\frac{\partial \mathbf{J}_p^{-1}}{\partial z_i}$ in terms of platform parameters and $\mathbf{z}$.

Next we are going to find out the expression of $\frac{\partial \mathbf{a}}{\partial z_j}$. For that we require the expressions of $\frac{\partial \mathbf{HF}}{\partial z_i}$, $\frac{\partial \eta_j}{\partial z_i}$ and $\frac{\partial}{\partial z_i}\begin{bmatrix}\Re_p\mathbf{F}_{ext}\\ \Re_p\mathbf{M}_{ext}\end{bmatrix}$.

$$\frac{\partial \mathbf{HF}}{\partial z_i} = \frac{\partial \mathbf{H}}{\partial z_i}\mathbf{F} + \mathbf{H}\frac{\partial \mathbf{F}}{\partial z_i} \tag{B.26}$$

where

$$(\frac{\partial \mathbf{H}}{\partial z_i})_{j\text{-th column}} = \begin{bmatrix}\frac{\partial \mathbf{s}_j}{\partial z_i}\\ (\frac{\partial \mathbf{q}_{p_j}}{\partial z_i}\times\mathbf{s}_j + \mathbf{q}_{p_j}\times\frac{\partial \mathbf{s}_j}{\partial z_i})\end{bmatrix} \quad j = 1 \text{ to } 6\ ; \tag{B.27}$$

$$\frac{\partial \mathbf{F}}{\partial z_i} = \begin{bmatrix}\vdots\\ K_{leg_j}\frac{\partial L_j}{\partial z_i}\\ \vdots\end{bmatrix}_{1\times 6}. \tag{B.28}$$

$$\frac{\partial \eta}{\partial z_i} = \frac{\partial \eta_{plat}}{\partial z_i} + \frac{\partial}{\partial z_i}\sum_{j=1}^{6}\eta_j \tag{B.29}$$

$$\frac{\partial \eta_{plat}}{\partial z_i} = \begin{bmatrix} M\{\frac{\partial \omega_p}{\partial z_i}\times(\omega_p\times\mathbf{R}_p) + \omega_p\times(\frac{\partial \omega_p}{\partial z_i}\times\mathbf{R}_p) + \omega_p\times(\omega_p\times\frac{\partial \Re_p}{\partial z_i}\mathbf{R}_{0_p})\} \\ \frac{\partial \omega_p}{\partial z_i}\times\mathbf{I}\omega_p + \omega_p\times\frac{\partial \mathbf{I}}{\partial z_i}\omega_p + \omega_p\times\mathbf{I}\frac{\partial \omega_p}{\partial z_i} \\ +M(\frac{\partial \Re_p}{\partial z_i}\mathbf{R}_{0_p})\times\{(\omega_p\cdot\mathbf{R})\omega_p - \mathbf{g}\} \\ +M\mathbf{R}_p\times\{(\frac{\partial \omega_p}{\partial z_i}\cdot\mathbf{R}_p)\omega_p + (\omega_p\cdot(\frac{\partial \Re_p}{\partial z_i}\mathbf{R}_{0_p})\omega_p) + (\omega_p\cdot\mathbf{R}_p)\frac{\partial \omega_p}{\partial z_i}\} \end{bmatrix} \tag{B.30}$$

$$\frac{\partial \eta_j}{\partial z_i} = \begin{bmatrix}\frac{\partial \mathbf{V}_j}{\partial z_i}\\ \frac{\partial \mathbf{q}_{p_j}}{\partial z_i}\times\mathbf{V}_j + \mathbf{q}_{p_j}\times\frac{\partial \mathbf{V}_j}{\partial z_i} - \frac{\partial \mathbf{f}_j}{\partial z_i}\end{bmatrix} \tag{B.31}$$

Expression of $\frac{\partial \mathbf{V}_j}{\partial z_i}$ has been developed later. Other terms of Eqn. (B.29), (B.30) and (B.31) have already been found out.

$$\frac{\partial}{\partial z_i}\begin{bmatrix} \Re_p \mathbf{F}_{ext} \\ \Re_p \mathbf{M}_{ext} \end{bmatrix} = \begin{bmatrix} \frac{\partial \Re_p}{\partial z_i}\mathbf{F}_{ext} \\ \frac{\partial \Re_p}{\partial z_i}\mathbf{M}_{ext} \end{bmatrix} \tag{B.32}$$

Expression of $\frac{\partial \mathbf{a}}{\partial z_i}$ can be found out using (B.26), (B.29) and (B.32).

Hence we have got the expression for Jacobian matrix ($\mathbf{A}$), in terms of Stewart platform parameters and $\mathbf{z}$.

$$\frac{\partial \dot{\mathbf{S}}_j}{\partial z_i} = \frac{\partial \omega_p}{\partial z_i} \times \mathbf{q}_{p_j} + \omega_p \times \frac{\partial \mathbf{q}_{p_j}}{\partial z_i} + \frac{\partial \dot{\mathbf{t}}_{p_j}}{\partial z_i} \tag{B.33}$$

$$\frac{\partial \mathbf{W}_j}{\partial z_i} = \frac{1}{L_j^2}\{L_j(\frac{\partial \mathbf{s}_j}{\partial z_i} \times \dot{\mathbf{S}}_j + \mathbf{s}_j \times \frac{\partial \dot{\mathbf{S}}_j}{\partial z_i}) - \frac{\partial L_j}{\partial z_i}(\mathbf{s}_j \times \dot{\mathbf{S}}_j)\} \tag{B.34}$$

$$\frac{\partial \dot{L}_j}{\partial z_i} = \frac{\partial \mathbf{s}_j}{\partial z_i}.\dot{\mathbf{S}}_j + \mathbf{s}_j.\frac{\partial \dot{\mathbf{S}}_j}{\partial z_i} \tag{B.35}$$

$$\frac{\partial \mathbf{U}_{1_j}}{\partial z_i} = \frac{\partial \omega_p}{\partial z_i} \times (\omega_p \times \mathbf{q}_{p_j}) + \omega_p \times (\frac{\partial \omega_p}{\partial z_i} \times \mathbf{q}_{p_j}) + \omega_p \times (\omega_p \times \frac{\partial \mathbf{q}_{p_j}}{\partial z_i}) \tag{B.36}$$

$$\begin{aligned}\frac{\partial u_j}{\partial z_i} = {} & (\frac{\partial \mathbf{s}_j}{\partial z_i}.\mathbf{U}_{1_j} + \mathbf{s}_j.\frac{\partial \mathbf{U}_{1_j}}{\partial z_i}) + \frac{1}{L_j^2}[\{(\frac{\partial \dot{\mathbf{S}}_j}{\partial z_i} - \frac{\partial \dot{L}_j}{\partial z_i}\mathbf{s}_j - \dot{L}_j\frac{\partial \mathbf{s}_j}{\partial z_i})^T(\dot{\mathbf{S}}_j - \dot{L}_j\mathbf{s}_j) \\ & +(\dot{\mathbf{S}}_j - \dot{L}_j\mathbf{s}_j)^T(\frac{\partial \dot{\mathbf{S}}_j}{\partial z_i} - \frac{\partial \dot{L}_j}{\partial z_i}\mathbf{s}_j - \dot{L}_j\frac{\partial \mathbf{s}_j}{\partial z_i})\}L_j - (\dot{\mathbf{S}}_j - \dot{L}_j\mathbf{s}_j)^2\frac{\partial L_j}{\partial z_i}]\end{aligned} \tag{B.37}$$

$$\begin{aligned}\frac{\partial \mathbf{U}_{2_j}}{\partial z_i} = {} & \frac{1}{L_j^2}[\{\frac{\partial \mathbf{s}_j}{\partial z_i} \times \mathbf{U}_{1_j} + \mathbf{s}_j \times \frac{\partial \mathbf{U}_{1_j}}{\partial z_i} - 2(\frac{\partial \dot{L}_j}{\partial z_i}\mathbf{W}_j + \dot{L}_j\frac{\partial \mathbf{W}_j}{\partial z_i})\}L_j \\ & -\frac{\partial L_j}{\partial z_i}(\mathbf{s}_j \times \mathbf{U}_{1_j} - 2\dot{L}_j\mathbf{W}_j)]\end{aligned} \tag{B.38}$$

$$\begin{aligned}\frac{\partial \mathbf{U}_{3_j}}{\partial z_i} = {} & \frac{\partial \mathbf{U}_{2_j}}{\partial z_i} \times \mathbf{r}_{d_j} + \mathbf{U}_{2_j} \times \frac{\partial \mathbf{r}_{d_j}}{\partial z_i} + \frac{\partial \mathbf{W}_j}{\partial z_i} \times (\mathbf{W}_j \times \mathbf{r}_{d_j}) \\ & +\mathbf{W}_j \times (\frac{\partial \mathbf{W}_j}{\partial z_i} \times \mathbf{r}_{d_j}) + \mathbf{W}_j \times (\mathbf{W}_j \times \frac{\partial \mathbf{r}_{d_j}}{\partial z_i})\end{aligned} \tag{B.39}$$

$$\begin{aligned}\frac{\partial \mathbf{U}_{4_j}}{\partial z_i} = {} & \frac{\partial u_j}{\partial z_i}\mathbf{s}_j + u_j\frac{\partial \mathbf{s}_j}{\partial z_i} + \frac{\partial \mathbf{U}_{2_j}}{\partial z_i} \times \mathbf{r}_{u_j} + \mathbf{U}_{2_j} \times \frac{\partial \mathbf{r}_{u_j}}{\partial z_i} + \frac{\partial \mathbf{W}_j}{\partial z_i} \times (\mathbf{W}_j \times \mathbf{r}_{u_j}) \\ & +\mathbf{W}_j \times (\frac{\partial \mathbf{W}_j}{\partial z_i} \times \mathbf{r}_{u_j}) + \mathbf{W}_j \times (\mathbf{W}_j \times \frac{\partial \mathbf{r}_{u_j}}{\partial z_i}) + 2(\frac{\partial \dot{L}_j}{\partial z_i}\mathbf{W}_j \times \mathbf{s}_j \\ & +\dot{L}_j\frac{\partial \mathbf{W}_j}{\partial z_i} \times \mathbf{s}_j + \dot{L}_j\mathbf{W}_j \times \frac{\partial \mathbf{s}_j}{\partial z_i})\end{aligned} \tag{B.40}$$

$$\begin{aligned}\frac{\partial \mathbf{U}_{5_j}}{\partial z_i} = {} & m_{dj}(\frac{\partial \mathbf{r}_{d_j}}{\partial z_i} \times \mathbf{U}_{3_j} + \mathbf{r}_{d_j} \times \frac{\partial \mathbf{U}_{3_j}}{\partial z_i}) + m_{uj}(\frac{\partial \mathbf{r}_{u_j}}{\partial z_i} \times \mathbf{U}_{4_j} + \mathbf{r}_{u_j} \times \frac{\partial \mathbf{U}_{4_j}}{\partial z_i}) \\ & +(\frac{\partial \mathbf{I}_{d_j}}{\partial z_i} + \frac{\partial \mathbf{I}_{u_j}}{\partial z_i})\mathbf{U}_{2_j} + (\mathbf{I}_{d_j} + \mathbf{I}_{u_j})\frac{\partial \mathbf{U}_{2_j}}{\partial z_i} + \frac{\partial \mathbf{W}_j}{\partial z_i} \times (\mathbf{I}_{d_j} + \mathbf{I}_{u_j})\mathbf{W}_j\end{aligned}$$

$$+\mathbf{W}_j \times (\frac{\partial \mathbf{I}_{d_j}}{\partial z_i} + \frac{\partial \mathbf{I}_{u_j}}{\partial z_i})\mathbf{W}_j + \mathbf{W}_j \times (\mathbf{I}_{d_j} + \mathbf{I}_{u_j})\frac{\partial \mathbf{W}_j}{\partial z_i}$$

$$-(m_{dj}\frac{\partial \mathbf{r}_{d_j}}{\partial z_i} + m_{uj}\frac{\partial \mathbf{r}_{u_j}}{\partial z_i}) \times \mathbf{g} + C_{uj}\frac{\partial \mathbf{W}_j}{\partial z_i} + \frac{\partial \mathbf{f}_j}{\partial z_i} \quad \text{(B.41)}$$

$$\frac{\partial \mathbf{V}_j}{\partial z_i} = \{m_{uj}(\frac{\partial \mathbf{s}_j}{\partial z_i}.\mathbf{U}_{4_j} + \mathbf{s}_j.\frac{\partial \mathbf{U}_{4_j}}{\partial z_i}) + C_{pj}\frac{\partial \dot{L}_j}{\partial z_i} - m_{uj}\frac{\partial \mathbf{s}_j}{\partial z_i}.\mathbf{g}\}\mathbf{s} - \frac{1}{L_j^2}\{L_j(\frac{\partial \mathbf{s}_j}{\partial z_i} \times \mathbf{U}_{5_j}$$

$$+\mathbf{s}_j \times \frac{\partial \mathbf{U}_{5_j}}{\partial z_i}) - \frac{\partial L_j}{\partial z_i}(\mathbf{s}_j \times \mathbf{U}_{5_j})\} + (m_{uj}\mathbf{s}_j.\mathbf{U}_{4_j} + C_{pj}\dot{L}_j - m_{uj}\mathbf{s}_j.\mathbf{g})\frac{\partial \mathbf{s}_j}{\partial z_i} \quad \text{(B.42)}$$